Journal of Materials Chemistry A

Accepted Manuscript

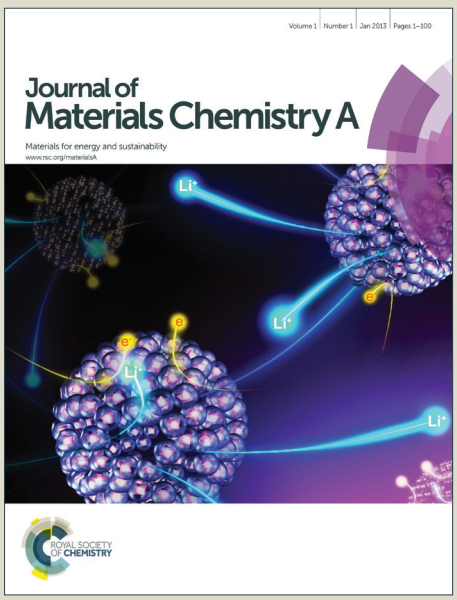

ROYAL SOCIETY OF CHEMISTRY

www.rsc.org/materialsA

Luminescent solar concentrators: Challenges for lanthanide-based organic-inorganic hybrid materials

Sandra F. H. Correia,[a,b] Verónica de Zea Bermudez,[c] Sidney J. L. Ribeiro,[d] Paulo S. André,[e] Rute A. S. Ferreira,*[a] Luís D. Carlos*[a]

[a] Physics Department and CICECO, University of Aveiro, 3810-193 Aveiro, Portugal. E-mail: lcarlos@ua.pt; rferreira@ua.pt; Tel: +351 234 370 946; Fax:+351 234 378 197.

[b] Instituto de Telecomunicações, Campus Universitário de Santiago, 3810-193 Aveiro, Aveiro, Portugal. Tel: +351 234 377 900; Fax: +351 234 377 901.

[c] Department of Chemistry and CQ-VR, University of Trás-os-Montes e Alto Douro, 5001-801 Vila Real, Portugal. Tel: +351 259 350 253; Fax: +351 259 350 480.

[d] Institute of Chemistry, São Paulo State University, UNESP, C.P. 355, 14801-970, Araraquara-SP, Brazil. Tel.: +551 633 019 631; Fax: +551 633 019 636.

[e] Instituto de Telecomunicações and Department of Electrical and Computer Engineering, Instituto Superior Técnico, University of Lisbon, Av. Rovisco Pais, Lisboa 1049-001, Portugal. Tel.: +351 218 418 486; Fax: +351 218 499 242.

Abstract

Luminescent solar concentrators (LSCs) are devices comprising a transparent matrix embedding optically active centres that absorb the incident radiation, which is re-emitted at a specific wavelength and transferred by total internal reflection to photovoltaic (PV) cells located at the edges of the matrix. Organic-inorganic hybrids incarcerating trivalent lanthanides ions (Ln^{3+}) are a very promising class of materials for addressing the required challenges in the LSCs design to improve solar energy

harvesting and, then, PV energy conversion. This feature article offers a general overview of the potential of down-shifting-based Ln^{3+}-containing organic-inorganic hybrids for the development of the area with special focus on i) optically active layer design, ii) energy conversion mechanisms, iii) performance and geometry and iv) figures of merit in PV cell enhancement. Finally, a prospective outlook on future progresses, e.g. optically active centres alignment, geometry optimization and building integration, is provided. The use of Ln^{3+}-containing hybrids in LSCs is at an infant initial research step and considerable basic knowledge is still needed to enable prototypes to become a commercial reality.

1. Introduction

The increase in the world's population and the growing demand for comfort have caused an enormous increment in energy consumption over the last 150 years, making the depletion of fossil fuels predictable in the midterm.[1] It is, then, imperative to use alternative forms of energy, namely natural and renewables ones that minimize CO_2 emissions. Solar energy has great potential because solar irradiation on Earth is 14 000 times higher than world's energy consumption and, if stored for a year, it becomes superior to the energy delivered by any of the fossil fuels.[1] Despite the development of photovoltaic (PV) systems over the last decades, the conversion of solar energy into electricity is not efficient enough and cost-competitive yet.[2]

The most efficient PV cells are based on III-V semiconductors,[3] such as GaAs (efficiency of ~29 %)[4] and multi-layered structures of GaAs, GaInP, InGaAs, GaInNAs and Ge (efficiency of up to ~43 %) that are, however, too expensive to become competitive.[4] Although presenting lower efficiencies, the most common PV cells are based on single crystalline Si (c-Si), polycrystalline Si (p-Si) and amorphous Si (a-Si)

(efficiencies of ~25, ~15 and ~10%, respectively).[3, 4] All-organic and dye-sensitized PV cells are emerging classes that have the potential to compete with Si-based ones in terms of efficiency under diffuse light conditions, which is a significant advantage for integration in urban buildings.[5] These cells still, however, display low efficiencies (maximum efficiencies of 8.6[6] and 12.3%[7], for all-organic and dye-sensitized solar cells, respectively) and high fabrication cost, compared to the Si-based cells.

Let us focus our attention on the c-Si PV cells, the efficiency of which is nowadays very close to the theoretical maximum established by the Shockley-Queisser limit of 32%.[8] One of the major factors limiting this efficiency is the mismatch between the solar spectrum and the Si band gap.[2] Fig. 1 shows the standard solar irradiance spectrum (AM1.5G, the detailed definition can be found, for instance, in Bünzli and Chauvin[3]) and the fractions of the total energy available for down-conversion (DC) and/or down-shifting (DS) (~16%) and up-conversion (UC) processes (~17%). The claimed improvements in the conversion yield of Si-based cells obtained by altering the cell architecture with trivalent lanthanide ions (Ln^{3+})-containing materials range from 0.3 to 2% (Table 9 of Bünzli and Chauvin[3]). Another drawback that limits the PV cells efficiency and the effective usage of the remaining solar energy is the fact that sunlight is diffuse and exists in a non-concentrated form, requiring the use of large mirrors to track the solar energy and direct the radiation to the cell. Besides increasing the cost, these mirrors are often large, demanding additional cooling, and care in their assembly must be taken to avoid shadowing regions in the cell.[9] Further increasing on the PV cells efficiency without external devices would be very difficult.

One way to cope with the above problems is through the usage of luminescent solar concentrators (LSCs). LSCs consist of a film (or layer) containing optically active centres, that, when exposed to light, convert part of the absorbing radiation into a

specific emitting wavelength. Part of the emitted signal will be lost at the surface (as detailed below) and the rest will be trapped inside the layer through total internal reflection that will guide it to the edges, where it can be collected by a PV cell, Fig. 2. This process endows a LSC with the ability of concentrating the maximum amount of light energy at its edges for electrical power generation. The light available at the edges of a LSC depends on: (1) The total surface area of the layer; (2) The total amount of incident light collected on the layer; (3) The type of layer; and (4) The quantum efficiency of the active species. The most widely used optically active centres in the emissive layer of LSCs are organic dyes, quantum dots (QDs), transition metals and Ln^{3+} ions. Moreover, the usage of LSCs boosts the reduction of the area of the PV cell (with the consequent reduction of the amount of material used), decreasing, therefore, the cost associated with energy conversion.[10] Nevertheless, it is estimated that LSCs will only be economically viable if the cost per Watt-peak generated can be reduced to about 1€/Watts-peak, meaning that the ratio between the cost of the LSC itself and the cost of the PV material in use should be <1/5.[11]

Despite the simple mechanism behind the LSC working principle, several factors must be taken into consideration while designing efficient devices. The first issue is related with the type of the target PV cell, in particular the energy band gap of the material that is used to produce the PV cell. The knowledge of the material band gap will determine both the sunlight wavelength region not absorbed by the PV cell and the wavelength emission range of the LSC emissive layer. To be effective in this application the optically active centres in the emissive layer (organic dyes, QDs, transition metals and Ln^{3+} ions) should present:[12]

- Broad spectral absorption;
- High absorption efficiency over the whole absorption spectrum;

- Large Stokes shift;
- High luminescence efficiency;
- Emission energy resonant with the PV-cell responsivity (input–output gain)

The first LSCs (initially termed as fluorescent/luminescent collectors) reported by W. Weber and J. Lambe in 1976, included active layers of Nd^{3+}- or Rhodamine 6G-doped glasses.[13] This work was followed by the theoretical study of A. Goetzberger and W. Greubel pointing out that concentration factors (ratio between the light emitted at surface and guided to the edges) around 100 appeared feasible.[6] In the following year, R. Reisfeld and S. Neuman announced the fabrication of LSCs made of uranyl-doped glass[14] whose performance was later improved by R. Reisfeld and Y. Kalisky in 1980 through the incorporation of Nd^{3+} and Ho^{3+} ions.[15] The presence of the Ln^{3+} ions induced an increased conversion efficiency with respect to that observed in LSCs based solely on uranyl-doped glass[14] because the energy absorbed by the uranyl group could be efficiently transferred to the Nd^{3+} and Ho^{3+} ions that emit in the near infrared (NIR) spectral range, closer to the maximum sensitivity of the c-Si PV cells.[15] Transition metal utilization was reviewed by Reisfeld and Jørgensen[16] and Reisfeld[17] in the 1980s.

A substantial increase in the LSCs research occurred over the past three decades, with the major advances of the field highlighted in several reviews published in the last five years. Key concepts related with loss sources (*e.g* reabsorption and escape cone) and the role of long term photostability, a crucial issue common to distinct optical species, was discussed by B. Rowan *et al.*[18] Another approach pointed out is the usage of NIR emitting QDs, despite the low intrinsic emission quantum yields which are still a severe drawback. According to these authors, challenges for organic-inorganic hybrids are envisaged, because it is unlikely that a single organic or inorganic material can

overcome the losses issues, the integration of the positive characteristic of each one into a hybrid material being considerably more attractive.[18] In fact, the properties of organic-inorganic hybrid materials are not just the sum of the individual contributions of both organic and inorganic phases and the role of their inner interfaces is predominant.[19]

The optical losses associated with a LSC were further reviewed in more recent works. For instance, R. Reisfeld,[20] reported the use of an organic-inorganic hybrid ormocer matrix to incorporate luminescent dyes in order to enhance the dye optical properties, namely reduce the reabsorption and increase the photostability. Other works discussed the possibility of maximising the light trapped inside the substrate through the application of selective mirrors that will reflect the light emitted at the surface back inside the substrate.[12] Photonic structures constructed at the surface of the LSC were also employed to increase the trapping efficiency.[20] The increase of the emission quantum yield was also discussed by using plasmonic structures.[12]

Several other works focused on the emitting species. For example, a review on the role of QDs as emitting species for LSC applications emphasized that the low quantum yields measured in organic matrices, large emission-absorption overlaps, unknown photostability and toxicity are still relevant issues to be addressed.[21] The incorporation of multiple stacks in which organic (dyes) and inorganic (QDs) species are joint together may result in an enlargement of the absorption range to achieve efficiencies well above 10%.[11]

J.-C. G. Bünzli and A.-S. Chauvin[3] reviewed recently the work done on the role of Ln^{3+} ions in PV systems. The energy conversion mechanisms are explained and their role in improving the solar energy conversion efficiency described and proven. A quantitative general assessment is made predicting that improvements on the order of 5% in conversion yield are feasible.[3]

The present review intends to summarize the work done in LSCs based on organic-inorganic hybrid materials reported in the literature over the last years. Despite the potential for generating low-cost solar power, LSC development faces various challenges, most of which related to the materials used in their design,[18] and various authors (even since the very beginning of the field[16]) concluded that the combination of organic and inorganic counterparts into single hybrid materials should play a key role on the design optimization.[3, 15, 17] Moreover, despite the quite limited use of hybrid materials in the fabrication of LSC, their efficiency values (Table 1) are of the same order of magnitude as those of pure organic LSCs.[22-25] Besides the influence of materials design, the manuscript gives particular attention to how emission mechanisms (energy conversion) can be used to enhance the LSCs performance. Although the three distinct mechanisms DS, DC and UC can be involved in the solar energy conversion, to the best of our knowledge, only LSCs based on DS hybrid materials have been reported until now. Therefore, we will devote this review paper to such examples. Moreover, there are a lot of publications that only highlight the potential role of organic-inorganic hybrid materials in LSCs without any device quantification performance. This review will not cover these examples.

2. Materials Design

The active layer – sometimes called substrate – is a key component of LSCs. It is usually a layer of glass or a sheet of a polymer within which the active species are *dispersed* (or encapsulated). The term *dispersed* regards here dispersion, dissolution, doping, or emulsifying. Owing to their high transparency and durability under exposure to sunlight,[26, 27] polycarbonate (PC) and PMMA thermoplastics have been the most

extensively employed polymers in the fabrication of sheets for LSCs. Thermoplastic copolymers are also considered to be good candidates for this purpose.[28]

In a very recent work, Buffa *et al*.[29] demonstrated the potential of substrates based on the PS rubber for the production of flexible LSCs offering sizable benefits and extended applicability with respect to standard, rigid LSCs (Fig. 3). The efficiency of light collection of PS rubbers doped with the Lumogen Red 305 (LR305) BASF fluorescent dye at different concentrations was comparable to that of PC substrates with the same dye concentration. Unlike in PC-based substrates, in PS-based substrates a LR305 concentration of 0.01% weight was the upper limit beyond which self-absorption and quenching effects took place with detrimental consequences on light output (for PC this value is 0.05 wt%). The dissimilar behaviour of LR305 in PS and PC at higher concentration was associated with the lower solubility of the dye in the apolar environment of PS.

Bhaumik *et al.*[28] developed a LSC composed of a dual-layer sheet or panel operatively connected to a light energy converter. The sheet comprised a first layer composed of a polymer in which a fluorescent dye (a perylene, a daylight fluorescent dye with a maximum absorption wavelength of 600 nm and a maximum emission wavelength range between 600 to 650 nm) was "dispersed" and a second layer comprising the second polymer in which a dye compound (quantum efficiency of more than 80%, a maximum absorption wavelength between 600 and 650 nm and a maximum emission wavelength of 650 nm, or greater) was also "dispersed". Both dyes absorbed light and radiated the absorbed light at longer wavelengths. A fluorescent brightener was also included together with the fluorescent dye, since the dye combination led to an increase of the emissions intensity. Typically the concentration of the dyes ranged from 0.001 to 1.0 weight %. Both layers were made of PC, with a light transmittance greater

than 55%, or PMMA. This design enabled the transmission of light radiated from the first fluorescent dye and the dye compound to the light energy converter. Such "dye cascade" approach allowed capturing more of the light energy to which the sheet was exposed. The sheet, with dimensions 60 mm × 60 mm × 3.2 mm, exhibited an edge emission output of at least 450 W/m^2 when exposed to a radiation intensity of ca. 1000 W/m^2. The LSC could alternatively include a reflective backing layer.

The emitting centres used on LSC applications are also one crucial factor for its efficiency and so, the choice must be done carefully. Comparing different emitting centres, organic dyes present the highest solubility in water and organic solvents,[30] the highest emission quantum yields (above 80%) and largest absorption coefficients.[12] The most common dyes used for LSC are rhodamines,[13, 31-37] coumarins,[24, 32, 33, 35-39] and perylene (bisimide) derivatives.[24-26, 37-46] The main drawbacks related with the use of organic dyes are the small Stokes shift (<50 nm) and photobleaching. In particular, the latter effect determines the lifetime of the LSC and occurs when a fluorophore permanently loses the ability to fluoresce due to photon-induced chemical damage and covalent modification.[47]

Another class of emitting centres includes QDs. The quantum confinement effect describing the dependence of the absorption wavelength on their particle sizes are of particular interest. It is possible to tune the absorption spectra using different semiconductor materials of different sizes.[21] Besides, there is the possibility of fabricating QDs with core-shell structure, in which the QD used in the core has a band gap energy different from that of the shell[48]. The emission quantum yields vary within 10-80%[30, 49, 50] and the main drawbacks are connected with the possible toxicity and photoblinking. The photoblinking mechanism results in an "*on-off*" emission behaviour

that would be disadvantageous for LSC applications since the device performance would not be constant over time.[51-55]

Transition metal ions display absorption spectra spanning the ultraviolet-visible (UV-VIS) spectral range with broad and sometimes strong intraconfigurational *d-d* transitions. Emission is also observed for some of them (Cr^{3+}, Mn^{2+} and Fe^{3+} for example) and application in LSC is therefore foreseen. Although the first papers stressing the potential application in LSCs were published in the 1980s,[16, 17, 56] very few works were published ever since.[57]

Ln^{3+} ions, usually coordinated to organic ligands to enhance the intrinsic *f-f* low-absorption cross-section,[19] are good candidates for applications in LSCs, not only because of their large Stokes shift (>200 nm), compared to those of organic dyes or QDs, but also because of their relatively high emission quantum yields. The challenge is the choice of the best ligand that enhances the Ln^{3+} emission (through the optimization of the balance between the ligands absorption, generally in the UV range, ligand-to-Ln^{3+} energy transfer and non-radiative deactivations). The highest quantum yield values ever reported, ~80%, being for Eu^{3+} β-diketonate complexes.[58-61] Ln^{3+} complexes can also be incorporated into organic-inorganic hybrid materials favouring the photostability of the active centres[60, 62] and permitting the easy process as thin films.[63-77] Moreover, despite the fact that in general complex incorporation is disadvantageous from the emission quantum yield point of view, there are some examples in which the emission quantum yield is preserved after the incorporation of the Ln^{3+} complex into hybrid matrices.[78, 79]

The intensity of the emitting centres may be enhanced through the use of metallic nanoparticles (NPs), *e.g.* silver (Ag) and gold (Au), due to the surface plasmon resonance effect.[80-87] In particular, it was demonstrated that the transition probabilities

from the ground to the excited state of dyes are favoured by the interaction of the electronic state of the dye with metallic plasmons[20] and the increase of emission of dyes in presence of Ag NPs in sol–gel organic-inorganic hybrid films was reported.[87-94] The presence of Ag NPs on collection efficiency of luminescent plate increases 12%, when compared with identical plate without them.[20] Luminescence intensification of lanthanide complexes by Ag NPs incorporated in organic-inorganic hybrids was also demonstrated.[88, 89] For instance, zirconia-GLYMO films doped with Eu^{3+} complexes show an intra-$4f^6$ fluorescence enhancement of 289–440% depending on the concentration of Ag NPs.[89]

3. LSC emission mechanisms

Energy conversion, through DS, DC and UC mechanisms is one of the attractive properties displayed by Ln^{3+}-doped materials, as mentioned above. Since the seminal work performed in the 1960s on UC, the energy transfer process involving different Ln^{3+} ions has been explored, with many different applications being proposed.[95-101] Concerning PV cells, Ln^{3+}-based up-converters have been observed to lead to efficiency enhancement. Some of the examples include: GaAs with a GeO_2-PbF_2 vitroceramic doped with Er^{3+} and Yb^{3+},[102] c-Si with $NaYF_4:Er^{3+}$,[103] a-Si with $NaYF_4:Yb^{3+}(18\%)Er^{3+}(2\%)$[104] and also dye-sensitized solar cells using $Y_3Al_5O_{12}$ transparent ceramics containing $Yb^{3+}(3\%)$ and $Er^{3+}(0.5\%)$[105] or Er^{3+}/Yb^{3+} co-doped LaF_3-TiO_2.[106] Most of the UC materials used for enhancing PV cells efficiency are Ln^{3+}-based NPs dispersed in polymers (e.g. PMMA[104, 107] or acrylic adhesive medium[108, 109]) or organic-inorganic matrices (e.g. polydimethylsiloxane, PDMS)[110, 111] to make possible the deposition on the PV cells surface.

In UC, one high-energy photon (typically in the UV-VIS regions) is emitted after excitation of the sample by two (or more) low-energy photons (typically in the IR region). Efficient energy transfer rates and phonon energy of the host are key features in this energy conversion efficiency. Energy transfer rates are directly connected to the overall efficiency of the conversion process, while phonon energy is closely related to multiphonon relaxation of excited levels. Particular interest involves low phonon energy hosts with the consequent decrease in multiphonon relaxation for Ln^{3+} excited levels. Fluoride and chalcogenide hosts (crystals or glasses) are indeed attractive hosts concerning energy conversion.

General properties of Ln^{3+} ions (namely UC) in fluoride and chalcogenide glasses have been extensively explored.[112, 113] Interesting examples are the fluorozirconate glasses (mainly based on ZrF_4, BaF_2, LaF_3, AlF_3 and NaF) and the fluoroindates glasses (mainly based on InF_3, ZnF_2, BaF_2 and SrF_2). For example, for the latter, energy UC has been observed in single-doped (Er^{3+},[114-116] Nd^{3+},[117, 118] Pr^{3+},[119] Ho^{3+},[118] Tm^{3+}[118]) and also co-doped (Yb^3/Ho^{3+},[120] Yb^{3+}/Tb^{3+},[118, 121] Yb^{3+}/Pr^{3+},[122, 123] Yb^{3+}/Tm^{3+},[124-126] Pr^{3+}/Nd^{3+} [118]) samples.

Materials showing UC, potentially useful for PV cells, have been reviewed by several groups worldwide.[97, 101, 127-129] Comprehensive tables comprising several low phonon hosts (crystalline or amorphous) for which efficient Ln^{3+} UC is observed were reported by Wang and Liu[97] and Strümpel *et al.*,[128] whereas the hosts effectively tested in PV cells were reviewed by Wang *et al.*[127] and de Wild *et al.*[129] Of particular interest are the $NaYF_4$:Ln^{3+} NPs, mentioned in all the reviews.[94] The possibility of obtaining these NPs with controlled sizes and morphology[98, 130] leads to potential new applications, as, for instance, pH-induced thermally controlled drug release for in vivo bioimaging and cancer therapy.[131] Maximum quantum yields of 50% would be

expected, but only in rare examples this value is higher than 10%.[3] The published papers reporting UC energy conversion for c-Si PV cells show a small improvement in its efficiency (<1%).[112, 132]

In any case, we must remember that UC is a non-linear effect that can be efficient as long as very high power density excitation is provided. In fact all the papers cited above mention the utilization of monochromatic excitation. Under direct sunlight the process is in fact very inefficient. There are two approaches that consider increasing efficiencies. In the first one broad excitation bands are used.[133, 134] An enhancement of quantum efficiencies is observed in comparison to monochromatic excitation conditions because all the Er^{3+} transitions involved are excited resonantly. The second approach being investigated concerns the use of the plasmon resonance of metal NPs at the surroundings of the UC material. In fact large enhancement of UC of Er^{3+} with Au plasmon resonance was well demonstrated.[135] The utilization of this principle in solar cells was verified, both theoretically[136] and experimentally.[137]

DC is also possible to be observed in Ln^{3+}-containing materials. In DC one high-energy photon absorbed (typically in the UV-VIS region) is converted in two lower-energy photons (typically in the VIS-IR regions).[138] Among many possible applications, the one attracting special interest nowadays includes the application of down-converters in PV cells. In the case of c-Si-based cells, photons with energy above the Si band gap, otherwise converted in heat, could be split in low energy photons that will be converted in electricity.[139]

Ln^{3+}/Yb^{3+} couples have been proposed, where the energy absorbed by the Ln^{3+} ion in the UV-VIS region is down-converted to two or more nearby Yb^{3+} ions. The Yb^{3+} ion with its single excited state $^2F_{5/2}$ emits at round 1000 nm, close to the Si band-gap. This process was first demonstrated in Tb^{3+}/Yb^{3+} co-doped yttrium-phosphate hosts[140] but

other couples have been studied afterwards, such as, Pr^{3+}/Yb^{3+} [141-148], Tm^{3+}/Yb^{3+},[149] Ce^{3+}/Yb^{3+},[150] Er^{3+}/Yb^{3+},[151] and Nd^{3+}/Yb^{3+}.[152]

Theoretically, a quantum yield value of 200% could be achieved, but there are very few reports of well-succeeded DC experiments with PV cells, being 158% the maximum DC quantum yield reported for a c-Si PV cell equipped with a DC glass layer doped with Pr^{3+} and Yb^{3+} (Fig. 4).[153] Numerical modelling of a c-Si cell and a DC glass layer doped with Pr^{3+} and Yb^{3+} led to a DC quantum yield of 186%.[154]

All the examples mentioned above involve inorganic hosts. Organic hosts, with relatively high energy vibrational modes, are almost useless. However the organic-inorganic hybrid concept may be well applied in this field. Nanoparticulate systems may be incorporated into organic hosts while keeping the optical properties of the inorganic host. Ln^{3+} emission in the NIR spectral region, with potential application in optical amplification, is observed in organic-inorganic hybrids and several examples were reported in the last years.[19, 155-157]. UC in Er^{3+}/Yb^{3+}-containing hybrids is also observed under 980 nm excitation.[158, 159] Zou *et al.*[160, 161] introduced recently a breakthrough concept based on UC of NIR photons in hybrid materials that can eventually overcome the Shockley–Queisser efficiency limit of the PV cells. An organic NIR dye was used as an antenna for β-$NaYF_4$:Yb,Er NPs in which the UC process occurs and the overall UC by the dye-sensitized NPs was dramatically enhanced (by a factor of ~3.300) as a result of increased absorptivity and overall broadening of the absorption spectrum of the up-converter (Fig. 5).

4. Performance and geometry

The performance of a LSC is quantified by the optical conversion efficiency (η_{opt}) that is a measure of ratio between the output power (P_{out}) at the LSC edges and the incident optical power (P_{in}):[21, 22, 24, 162, 163]

$$\eta_{opt} = \frac{P_{out}}{P_{in}}. \quad (1)$$

The η_{opt} can be described by weighting all the losses (Fig. 2A) in the LSC, given by the product of several terms:[163]

$$\eta_{opt} = (1 - R)\eta_{abs}\eta_{SA}\eta_{yield}\eta_{Stokes}\eta_{trap}\eta_{tr} \quad (2)$$

in which:

- $R=(1-n_i)^2/(1+n_i)^2$ is the Fresnel reflection coefficient for perpendicular incidence, in which n_i represents the refractive index of the emitting medium at the incident wavelength (λ_i).
- $\eta_{abs}=1-10^{-A}$ is the ratio of photons absorbed by the emitting layer to the number of photons falling on it, with A representing the absorbance value at λ_i. For LSCs with a non-planar geometry, η_{abs} is not constant along the device surface and, then, the thickness must be estimated accordingly. For instance, for cylindrical geometry, and perpendicular incidence of sun radiation, the optical absorption path increases from the middle to the surface along the radial direction.[164]
- η_{SA} is the self-absorption efficiency, arising from self-absorption of the emitting centres. When the spectral overlap between the excitation and emission spectra of the

emitting centres is null, η_{SA}=1, as in the case of Ln^{3+}. If this overlap is not null, η_{SA}<1, as typically observed for dyes and QDs.

- η_{yield} is the emission quantum yield of the optically active centre at λ_i.
- $\eta_{Stokes}=\lambda_i/\lambda_p$, is the Stokes efficiency calculated by the energetic ratio between the average energy of the emitted photons (the emission peak position, λ_p, in energy units) and the incident energy (corresponding to λ_i).
- $\eta_{trap}=(1-1/n_p^2)^{1/2}$, the trapping efficiency, where n_p is the refractive index of the emitting medium at λ_p, is defined as the fraction of photons confined within the substrate, i.e., the fraction of photons emitted from the edge versus the photons emitted from the face and edge combined. This term accounts for the emission losses at the surface through a so-called escape cone with an aperture angle defined by $\theta_c=2\times sin^{-1}(1/n_p)$.[18]
- η_{tr} takes into account the transport losses due to matrix absorption and scattering, frequently it is considered that η_{tr}=1, as the transport and scattering losses are neglected.

We should call the attention to the fact that some of us recently reported that scattering plays an important role, which readily contributes to decrease η_{tr}.[76] In particular, the emission ratio C, defined as the ratio between the intensity at the surface and at the edges, was modelled by:

$$C = \frac{\eta_{opt}}{\frac{\eta_{sf}}{2}} \frac{A_{sf}}{A_e} = \frac{2\eta_t}{(1-\eta_t)} \frac{A_{sf}}{A_e} \quad (3)$$

where

$$\eta_{sf} = (1-R)\eta_{abs}\eta_f\eta_s\eta_t(1-\eta_{tr})\eta_{self} \quad (4)$$

is the conversion efficiency of the signal emitted at the surface of the film (in which the trapping efficiency is replaced by its complementary value, (1-η_t)), A_{sf} and A_e are the surface area and the area of the plate edges, respectively, and the factor ½ takes into account the emission regards only one film surface. The *C* factor predicted by eqn (4) should be compared with that measured experimentally.[76] Some of us demonstrated for LSCs based on bridged silsesquioxane hybrids doped with Eu^{3+} that the value estimated by eqn (4) was substantially higher (57) than the experimental value (6). Such discrepancy was explained by considering that the signal trapped in the waveguide will lose part of its intensity due to scattering effects along the propagation in the film (i.e. the scattered signal emitted by the surface), in a similar way that was performed in the estimation of the losses incurred by self-absorption in LSCs of liquid solutions of PbS QDs.[49] Therefore, eqn (3) was rewritten as follows:

$$C_{eff} = \frac{2\eta_{tr}\eta_t}{(1-\eta_t)+(1-\eta_{tr})}\frac{A_{sf}}{A_e}. \quad (5)$$

Although not mentioned in the literature, we should notice that η_{opt} is dependent on the excitation wavelength. Therefore, the calculus of the overall optical conversion efficiency through eqn (2) requires integration over the excitation spectrum limits (λ_1 and λ_2):

$$\eta_{opt} = \frac{1}{\lambda_2 - \lambda_1} \times \int_{\lambda_1}^{\lambda_2} (1 - R(\lambda))\eta_{abs}(\lambda)\eta_{yield}(\lambda)\eta_{Stokes}(\lambda)\eta_{trap}(\lambda)d\lambda\,, \qquad (6)$$

assuming $\eta_{SA}=\eta_{tr}=1$.[76, 163] Obviously, integration limits that lie outside the AM1.5G spectral range are not useful for PV conversion. In this sense, an effective optical conversion efficiency can be calculated replacing the limits in eqn (6) by those of the integral overlap[60] between the excitation and the AM1.5G spectra. The variation of the percentages of the AM1.5G solar irradiance (see Figure 12 of Bünzli and Chauvin[3]) points out that for excitation wavelengths between 280 and 300 nm only 0.15% is available for DS conversion and that between 280 and 400 nm that percentage increases to 4.6%. The η_{opt} values calculated through eqn (6) can be directly compared with those estimated by eqn (1) and represent a valuable tool to describe the performance of a LSC in the absence of a solar simulator. Table 1 lists the η_{opt} values reported for LSC based on organic-inorganic hybrids.

The predictable maximum limit for η_{opt} was theoretically studied[21, 36, 139-141] not taking into account the excitation wavelength dependence. For instance, efficiency calculations with conventional solar cell theory applied to LSCs in a stack of transparent sheets involving dyes and semiconductors (Ge, Si, GaAs) yield a theoretical maximum conversion efficiency of 0.3, although more realistic values around 0.20 have been mentioned under optimum conditions.[6] Monte-Carlo studies (taking into account the absorption and emission probabilities) on LSCs based on perylimide dyes embedded in GLYMO,[44] liquid solutions of Rhodamine B and Red305 encapsulated in glass tubes,[165] and commercial CdSe-CdTe QDs[166] were recently performed. Also, a mathematical assessment of LSCs accounting for all the intrinsic (size, shape, design and materials)

and extrinsic (geographical, seasonal and spectral distribution of solar radiation) factors that influence the performance of such devices was also reported.[16] In all these works, the main limiting factor is the high spectral overlap between emission and absorption spectra that yield maximum values of η_{opt} within 20-30%. The maximum limit for η_{opt} can be also inferred through a simpler analysis of eqn (2), considering that all the involved parameters can be near the unit, except η_{trap} and η_{Stokes}. For typical values of the refractive index around 1.5, η_{trap}~75% and for a wavelength shift from the UV/blue to the red spectral region around 690 nm (around the wavelengths at which the a-Si PV cells are more efficient)[3] η_{Stokes}~50%, the maximum predictable value for η_{opt} is ~40%.

Besides η_{opt}, another parameter that is also often used to quantify the performance of a LSC is the concentration factor:[21]

$$F = G \times \eta_{opt} \quad (6)$$

in which G is the geometrical gain factor $G=A_t/A_e$, where A_t is the top surface area and A_e is the edge surface area of the LSC (assuming all of the other faces with reflective coatings and a white diffuser on the rear side).[21] Given the importance of G, many researchers have studied and compared LSCs with distinct geometries. McIntosh *et al.*[167] made a theoretical comparison between square-planar and cylindrical LSCs, introducing and proposing a new geometry composed of various cylinders, one after another. They found that the optical concentration of a cylindrical LSC can be 1.9 times higher than that of the square-planar LSC of equivalent collection area and volume. If the new multi-cylindrical geometry was considered, a small increase in optical concentration was obtained for all angles of incidence of radiation, due do multiple reflections between subsequent cylinders. Inman *et al.*[168] fabricated both solid and

hollow cylindrical LSCs using NIR QDs of PbS in PMMA matrices (Fig. 6). Their results showed that the hollow structures can lead to higher absorption and less self-absorption, comparing to the solid cylindrical LSC, thus giving better performance results. Furthermore, for QDs-doped LSCs the influence of the geometry in the efficiency was modelled showing no substantial gain between three different shapes of LSCs: hexagonal, square and a right-angle triangle.[38] Taking advantage of the cylindrical geometry of PMMA-derived plastic optical fibers (POFs) and of the large Stokes shift typical of Eu^{3+} β-diketonate complexes, a zero self-absorption loss LSC was made with a POF doped with $Eu(tta)_3phen$ (tta=2- thenoyltrifluoroacetone and phen=1,10-phenanthroline). The cylindrical geometry provides a geometric gain up to ~1500 (for a typical diameter of 1 mm and a length of 1 m).[169] A recent study also reported that coated cylindrical LSCs are more efficient when compared to homogeneously doped ones.[170]

When the LSCs are coupled to a PV cell the optical conversion efficiency can be calculated by:[44]

$$\eta_{opt} = \frac{I_{sc}^{L} V_0^{L}}{I_{sc} V_0} \times \frac{1}{G} \times \frac{\eta_{PV}}{\eta_{solar}} \quad (7)$$

where η_{PV} is the PV cell efficiency at λ_p and η_{solar} is the average efficiency value of the cell with respect to the total solar spectrum.[44] The parameters I_{sc}^{L} and V_0^{L} stand for the short-circuit current and the open voltage, respectively, when the PV cell is coupled to the LSC under AM1.5G illumination. I_{sc} and V_0 represent the short-circuit current and the open voltage, respectively, when the PV cell is exposed to AM1.5G illumination (in the absence of the LSC). In the literature, eqn (7) is often presented in simplified formulations given by eqn (8) and eqn (9):[21, 22, 24, 49, 162, 165, 168]

$$\eta_{opt} = \frac{I_{sc}^{L}}{I_{sc}} \times \frac{R_{PV}}{R_{solar}} \times \frac{1}{G} \quad (8)$$

in which R_{PV} is the responsivity of the solar cell efficiency at λ_p and R_{solar} is the average responsivity value of the cell with respect to the total solar spectrum.

$$\eta_{opt} = \frac{I_{sc}^{L}}{R_{PV}} \times \frac{1}{S} \times \frac{1}{G} \quad (9)$$

where S is the input power density.

When the LSC coupled to a PV cell is put under simulated solar illumination, the overall power conversion efficiency, *PCE*, is defined as the ratio between the output electrical power and the input optical power, given by:

$$PCE = \frac{I_{sc} V_0}{S.A_t} \times FF \quad (10)$$

where I_{SC} is the short circuit current, V_{OC} is the open circuit voltage, FF is the fill factor of the PV cell, S is the irradiation intensity and A_t is the area of the LSC top surface.

5. Figures of merit in PV cell enhancement

To the best of our knowledge, UC and DC processes have not been used yet for LSCs based on hybrid materials. In this section DS-based examples are presented and reviewed in detail (Table 1). Optical conversion efficiency, power conversion efficiency, short-circuit current densities and the increase in the current of the PV cells will be used to quantify figures of merit of PV cells performance in the presence of LSCs.

Focusing our attention on the optical conversion efficiency, the larger values were found for hybrid materials containing dyes, e.g. perylimide incorporated into GLYMO

(18.8%), and QDs, e.g. CdSe/CdS/ZnCdS/ZnS in a mixture of oleic acid in lauryl methacrylate and ethylene glycol dimethacrylate (15.3%, Fig. 7).[171] The cylindrical hollow QD LSC made of PbS incorporated into PMMA (Fig. 6) showed a η_{opt}~6.5%[168] and CdSe/ZnS dispersed in polyurethane and then casted into PMMA moulds presented a maximum value of η_{opt}~2.1%.[50]

Substantial lower values (~0.3-1.4%) were found for PbS and CdSe/ZnS QDs dispersed in toluene sealed into quartz[49] and in glass.[165] Although in general the maximum η_{opt} values of dye-containing organic-based LSCs are similar to those listed in Table 1,[22-24] there are some examples reporting higher values, such as for instance dye-containing parylene films with a maximum η_{opt} value of ~22.6%.[22]

Using eqn (2) for selected excitation wavelengths (Table 1), values of η_{opt} ~9 % for $Eu(tta)_3$.ephen (ephen=5,6-epoxy-5,6-dihydro-[1,10] phenanthroline) embedded into a tri-ureasil hybrid[60] and η_{opt} ~8.8% for Tb^{3+}/SA-doped PVA/PMMA films[172] were found. Playing with the effect of the substituent position on the bipyridine ring in Eu^{3+}- and Tb^{3+}-bridged silsesquioxanes (M4 and M6 hosts)[76, 77] a maximum value of η_{opt}~4.3% was reported for the Eu^{3+}-based LSCs.[76] We should note that the values reported for Tb^{3+}/SA-doped PVA/PMMA and Eu^{3+}- and Tb^{3+}-bridged M4 silsesquioxane were obtained under excitation of 290 nm, a wavelength lying outside the AM1.5G spectral range and, then, not useful for PV conversion.

The performance of PV cells in the presence of LSCs was also reported using others figures of merit (besides η_{opt}). For PbS and CdSe/ZnS QDs dispersed in toluene sealed into quartz LSCs and CdSe/CdS/ZnCdS/ZnS QDs in a mixture of oleic acid dispersed in lauryl methacrylate and ethylene glycol dimethacrylate, tested with Si PV cells, power conversion efficiency values of 3.2%, 1.2% (full perimeter)[49] and 2.8% (single edge)[171], respectively, were obtained. For the latter case, the short-circuit current

was 95.7 mA.cm^{-2}.[171] The LSC based on PMMA and 3-aminopropyl triethoxysilane (APTES) returned a short-circuit current of 7.2 mA, when using a multi-crystalline Si PV cell. The PS rubber waveguides doped with dyes were tested with a Si photodiode and a GaAs PV cell. The short-circuit current densities ranged from 66 to 102 A.m^{-2}, for the Si photodiode, and from 158 to 214 A.m^{-2}, for the GaAs PV cell. The maximum power delivered was between 8 and 19 W.m^{-2} and 97 and 120 W.m^{-2}, for the photodiode and GaAs PV cell, respectively.[29] The ormosil-based LSC with Eu(phen)$_2$ allowed an increase in the PV current of the Si PV cell of about 10-15%, when compared to the bare cell.[173] The increase of a-Si PV cell performance attached to the ends of a squared LSC formed of a glass substrate (1 cm thick) coated by a tri-ureasil hybrid doped with Eu(btfa)$_3$(MeOH)$_2$]$_2$bpta$_2$[79] (Fig. 8) was also attained. A value of power conversion efficiency of 0.007% for single edge was attained.

These values (power conversion efficiency, short-circuit current densities and increase in the PV current of the Si PV cell) can be compared with those reported for organic LSCs made by QDs or Ln^{3+} complexes embedded into polymers. One illustrative example involves LSCs made by PVB-doped with Eu(tta)$_3$dpbt (dpbt=2-(N,N-diethylanilin-4-yl)-4,6-bis(3,5-dimethylpyrazol-1-yl)-1,3,3-triazine) and Eu(tta)$_3$phen complexes.[174] Values of power conversion efficiency of 0.0499 and 0.0441%, for single edge, and 0.176 and 0.200%, for full perimeter, respectively, were obtained for tests with c-Si PV cells. Short-circuit current densities of 0.150 mA.cm^{-2}, Eu(tta)$_3$phen, and 0.168 mA.cm^{-2}, Eu(tta)$_3$dpbt, were reported.[174]

Besides the use of LSCs, DS and UC layers (so-called DSL and UCL, respectively) have been also used to enhance the PV cell performance.[175] The layer containing the luminescent species is used as PV cell coating. In this case, the light emission is transmitted directly to the PV cell, without optical guidance. Potentially, the

performance of this solution can exceed the LSCs one, since the propagation losses are much smaller due to the inexistence of optical guidance (the trapping losses are identical).

Ln^{3+}- and QDs-containing hybrid DSL have been used to improve the short-wavelength response of PV cells. The coating of a Si PV cell with an Eu^{3+}-doped ormosil was tested with an increased performance of 18%, compared to the uncoated c-Si PV cell.[176] Another example is the improvement of the external quantum efficiency (EQE) of a InGaAs photodetector from 1.8 to 21% using a DSL consisting of PbS/CdS core/shell QDs embedded in PMMA (Fig. 9).[177] Likewise, a DSL with CdSe/CdS core/shell QDs mixed with PMMA provided an enlargement of the EQE of CdTe PV devices from 4 to 20%.[178] An intriguing example of a PV module multilayer coating in which the DSL is $Eu(tta)_3$phen encapsulated into a sol-gel derived silica glass reported the increase in short-circuit current density of 1.03 mA/cm^2, compared with the value measured in the absence of the DSL.[179]

The use of an UCL of Yb^{3+}/Er^{3+}-doped silicone gel increased the EQE of a bifacial Si PV cell in 5.9×10^{-6} %, demonstrating a better performance than using a spin-on oxide to embed the UC particles, with an increase in the EQE of 4.0×10^{-7} %.[180] The potential of PbS QDs to enhance the performance of the UCLs mentioned above was tested dissolving PbS QDs together with the UC particles, both in the spin-on oxide and in the silicone gel. The results showed that, in both cases, the UC performance is enhanced in the presence of the PbS QDs, with an improvement in the photocurrent detected of 60%, due to the increase of light coupling to Er^{3+} atoms.[180]

Analogous figures of merit can be reached using Ln^{3+}-containing polymers as DSL for PV cells. For instance, comparing the variation of the EQE of a c-Si PV cell uncoated, coated with undoped polyvinyl acetate (PVA) film and coated with Eu^{3}-

doped PVA films, the cell coated with DSL displays an increase in the short-circuit current density from 35.67 to 36.38 mA/cm^2, whereas the overall energy conversion efficiency increases from 16.05% to 16.37%.[181] Another example showed an increase in the total delivered power of a c-Si cell coated with a Eu^{3+}-doped PVA DSL, relatively to the case of undoped PVA coating.[182]

The role of the DS mechanism in the potential enhancement of the EQE of a PV cell was recently predicted.[183] This model attempts to estimate the EQE of a PV cell coated with a DS layer, demonstrating that two main factors must be maximized; the luminescent DS efficiency (η_{LDS}, efficiency of down-shifting absorbed photons and sending them towards the under-lying solar cell) that depends on the emitting layer properties (quantum yield, emission and absorption spectral range and, refractive index) and on the emission spectral matching between the DS emission spectrum and the PV cell EQE) (eqn 4 of ref. [183]). Fig. 4 of reference [183] exemplifies the values for these two parameters (η_{LDS} and EQE) experimentally accessed for distinct types of PV cells coated with distinct DS layers. Focusing our attention into the case of the mono-Si PV cell that is coated with the above mentioned Eu^{3+}-complexes[181] it is possible to infer that although a high ESM value is attained (~87%) for all the cases, the η_{LDS} parameter increases from 39 to 63% due to the different absorption and emission properties of the complexes, namely the absorption coefficient and the emission quantum yield.

6. Prospects and conclusions

The synergy between the intrinsic characteristics of sol-gel derived organic–inorganic hybrids and the luminescence PV conversion features of Ln^{3+} ions affords Ln^{3+}-containing hybrid materials real potential for applications in LSCs. These devices consist of a host transparent matrix with optically active centres incorporated where

incident radiation is absorbed by them, re-emitted at a specific wavelength and transferred by total internal reflection to PV cells located at the edges of the LSC matrix. Contrary to conventional sunlight collectors, both diffuse and direct radiation is concentrated and, thus, less PV material is necessary, which becomes an advantage. The field is, however, in its infancy and much remains to be investigated before prototypes become a commercial reality. We now summarise some of the research themes deserving particular attention.

a) Dye alignment. An attractive strategy that emerged very recently and represents an extraordinarily promising path to performance enhancement of dye-doped LSCs is dye alignment. This exciting concept, first introduced by Verbunt *et al.*,[184] led to several interesting technological advances, such as the development of LSCs in which the dye molecules are either perpendicularly aligned to the plane of the substrate[185] or in a linear fashion in the plane of the substrate.[184, 186] Anisotropic LSCs exhibit a series of benefits with regard to isotropic LSCs. As described above, in conventional dye-doped LSCs randomly oriented luminescent molecules embedded in a transparent substrate (or waveguide) absorb diffuse light incident on the substrate and collectively re-emit these photons isotropically at a lower energy. Approximately ~75% of the re-emitted photons are trapped in the substrate through total internal reflection (considering a refractive index ~1.5). A fraction of the absorbed photons is lost from the substrate if they are re-emitted above the critical angle through the face of the LSC, or scattered outside of the substrate. In anisotropic LSCs, η_{trap}, may be improved by increasing the fraction of re-emitted photons that are trapped in the substrate through the control of the orientation of the dye molecules.[184]

Mulder *et al.*[185] reported an increase of the η_{trap} value from 66% for randomly oriented LSCs, relying on a hybrid system composed of isotropic Coumarin 6 (1% solid

weight content) and host PMMA, to 81% for a vertically-aligned LSC employing the rod shaped dye molecule Coumarin 6 (1% solid weight content) and a homeotropic polymerizable liquid crystal mixture including a polymerizable nematic liquid crystal, homeotropic dopant molecules, and a photo-initiator. Orienting the molecules perpendicularly to the substrate weakens the absorption of the perpendicular incident radiation. To correct this, an external holographic diffuser was successfully used above the LSC to scatter the incident light (Fig. 10A). These authors demonstrated that the enhancement of η_{trap} was preserved for G up to 30. We note that an increase of G without compromising η_{trap} is a key factor to reduce the cost of solar electricity.

b) Linearly Polarized LSCs (LPLSCs). LPLSCs, in which the dye molecules are aligned in-plane with the substrate, represent another challenging approach, since they are expected to replace classical linear polarizers for light harvesting applications (e.g., portable devices with flat panel displays). The absorption of LPLSCs is linearly polarized, meaning that light is absorbed very strongly for polarizations parallel to the dipole moment of the dye molecules, but, in contrast, perpendicularly polarized light is transmitted, leaving the substrate. As a consequence, LPLSCs resemble ordinary polarizers. However, instead of dissipating the absorbed photons as heat, a LPLSC funnels the captured photons to photocell elements placed at the edges of the substrate (Fig. 10B). Mulder *et al.*[186] aligned Coumarin 6 linearly in the plane of a glass substrate using the same polymerizable liquid crystal host used in the vertically-aligned LSC described above. To improve the harvesting of indoor radiation across the VIS spectrum, a horizontally-aligned LSC hosting two dye molecules cascading in energy (Coumarin 6 and 4-dicyanomethyl-6-dimethylaminostiryl-4H-pyran) was also created. Up to 38% of the photons polarized on the long axis of the dye molecules could be coupled to the edge of the device with an order parameter of 0.52.

c) Surface losses. The major issue associated with current LSCs has to do with the low efficiency they present that still doesn't make them cost-competitive with electric energy obtained from fossil fuels, since an efficiency value of 30% would be needed to make LSCs a commercially viable solution. Great part of total losses is due to the escape cone of the matrix (radiation that escape through the surface of the matrix instead of being internally reflected) and re-absorption of the emitted photons by the luminescent entities themselves, caused by overlap of absorption and emission spectra. It is then imperative to search for new optically active centres and LSC configurations to reduce losses and, consequently, increase the efficiency of these devices. Periodic surface patterning of the photoluminescent emitting layer may be envisaged in order to reduce the light escape though the surface.[187] The patterning of the organic-inorganic hybrid host is easily achieved incorporating photo responsive species, e.g. Zr(IV) *n*-propoxide chelated with methacrylic acid, at the LSC surface.

d) Geometry. The LSC geometry is crucial for further improvements on the conversion efficiency. Despite the fact that most of the devices are planar, theoretical works suggest that cylindrical geometry allows an increase of the concentration factor (compared with planar structures), yielding more efficient LSCs.[167, 168, 188] For instance, the concentration factor of a cylindrical LSC can be twice higher than that of a square-planar LSC of equivalent collection area and volume, because the ratio between the absorption and collection areas is greater than that of the planar LSCs.[167] Also, when diffuse radiation is considered instead of direct one, the optical concentration is higher for cylindrical LSCs, which has great advantages in cloudy weather conditions, shaded locations and whenever direct irradiance is scarce or absent.[188] Recently, a luminescent concentrator PV system that embeds large scale, interconnected arrays of microscale Si solar cells (μ-cells) in thin matrix layers doped with luminophores was proposed as an

alternative to conventional LSC planar geometry.[189] The dimensions and designs of the μ-cells allow the capture of light not only through their top surfaces, but also through their sidewalls and bottom surfaces increasing further their power output by more than 300%.[189] This unusual LSC design offers improved performance compared with conventional layouts, and a variety of engineering options with particular value in ultrathin, lightweight and bendable systems.

e) Building integration. The LSCs development can also be seen as an attractive way of dropping the solar energy costs, as they can assist the urban integration of PV devices. The PV structure becomes part of the building itself such as, for instance, as windows, balancing contributions towards natural lighting, as well as creating electrically active elements and increasing the visual impact of the building.[190-192] The multicolored glass panels that adorn the exterior of MUSAC, the contemporary art museum of Castilla and León, in Léon, Spain, are a good example that illustrates the huge potential of this idea (Fig. 11), although in this case their functionality is simply aesthetic (they resemble the stained-glass windows of the León cathedral).

e) DC hybrid materials. DC Ln^{3+}-containing hybrid materials have not yet been successfully demonstrated, despite the potential addition of up to 7 absolute % to the conversion yield.[3]

f) DC and UC processes working together. This is a subject clearly unexplored. An interesting example involving a hybrid nanostructure formed by Gd_2O_3:Yb(2%)/Er(0.3%) NPs coated with the $Eu(dbm)_3$phen complex was reported by Singh *et al.*[159] The nanocomposite displays green and red UC, upon excitation at 976 nm, together with a red DS, when excited at 355 nm (ligands levels) or 521 nm ($^2H_{11/2}$ intra f^{11} level). Although the anticipated beneficial effects of combining DC and UC processes (in a single layer or in a multilayer structure) should be demonstrated, once

coupled to PV devices this type of materials might be able to improve the conversion yields of Si-based (dye-sensitized) solar cells by as much as 5-8 (5.5-6.5) absolute%.[3]

A short note about the potential supply disruption of lanthanides, or more generally rare earth elements, must be made before ending the review. These elements are crucial in the transition to a green economy, due to their essential role in a large variety of technologies (permanent magnets, lamp phosphors, catalysts, rechargeable batteries and photonics) and are, therefore, in high demand.[193, 194] The low concentration in which they are present in the earth's crust makes economic exploitation difficult and consequently the potential risk of a supply disruption is a present concern.[195, 196] Although that risk analysis lies completely outside the scope of this paper, the relatively small amount of these elements that are used for LSCs (the emissive organic and organic-inorganic hybrid layers contain typically an amount of Ln^{3+} ions less than 10-15%, in weight) makes that potential shortage not so problematic, relatively to what can be anticipated in other research areas.

In the last decade there has been a emerged and ignited interest in LSCs, quite overlooked since the pioneering works in the 1970s and 1980s, leading to a significant development in the design, modelling and performance of the devices. Moreover, new and more efficient emitting centres (dyes, QDs and, particularly, Ln^{3+}-based complexes and NPs) have been synthesised and embedded into polymer and organic-inorganic hybrid hosts. Future research should be directed towards the enlargement of the absorption range and the lowering of losses, absorption in the matrix and re-absorption,[11] to make LSCs market competitive and helping the necessary turnover of the world energy consumption scenario.

Acknowledgements

Funding was provided by Fundação para a Ciência e a Tecnologia (FCT), EU/FEDER COMPETE and Mais Centro-PORC, under contracts PEst–C/CTM/LA0011/2013, PTDC/CTM-BPC/112774/2009 and CENTRO-07-ST24-FEDER-002032. The support of COST Action MP1202 "Rational design of hybrid organic-inorganic interfaces" and LUMINET - European Network on Luminescent Materials (316906, FP7-PEOPLE-2012-ITN) project is also acknowledged. SFHC thanks FCT for a PhD grant (SFRH/BD/91263/2012) and LDC thanks CAPES (Brazil) by a fellowship within the Nanobiotec network "Produção de materiais nanoparticulados para processos baseados em imunocitoquímica".

References

1. S. C. W. Krauter, *Solar Electric Power Generation - Photovoltaic Energy Systems*, Springer Berlin Heidelberg, New York, 2006.
2. X. Huang, S. Han, W. Huang and X. Liu, *Chem. Soc. Rev.*, 2013, **42**, 173.
3. J.-C. G. Bünzli and A.-S. Chauvin, in *Handbook on the Physics and Chemistry of Rare-Earths*, eds. J.-C. G. Bünzli and V. K. Pecharsky, Elsevier B. V., Amsterdam, 2014, vol. 44, pp. 169-282.
4. M. A. Green, K. Emery, Y. Hishikawa, W. Warta and E. D. Dunlop, *Prog. Photovoltaics*, 2012, **20**, 606.
5. R. Harikisun and H. Desilvestro, *Sol. Energy*, 2011, **85**, 1179.
6. L. T. Dou, J. B. You, J. Yang, C. C. Chen, Y. J. He, S. Murase, T. Moriarty, K. Emery, G. Li and Y. Yang, *Nat. Photonics*, 2012, **6**, 180.
7. A. Yella, H. W. Lee, H. N. Tsao, C. Y. Yi, A. K. Chandiran, M. K. Nazeeruddin, E. W. G. Diau, C. Y. Yeh, S. M. Zakeeruddin and M. Gratzel, *Science*, 2011, **334**, 629.
8. W. Shockley and H. J. Queisser, *J. Appl. Phys.*, 1961, **32**, 510.
9. M. J. Currie, J. K. Mapel, T. D. Heidel, S. Goffri and M. A. Baldo, *Science*, 2008, **321**, 226.
10. H. Hernandez-Noyola, D. H. Potterveld, R. J. Holt and S. B. Darling, *Energ. Environ. Sci.*, 2012, **5**, 5798.
11. W. G. J. H. M. van Sark, *Renew. Energ.*, 2013, **49**, 207.
12. M. G. Debije and P. P. C. Verbunt, *Adv. Energ. Mater.*, 2012, **2**, 12.
13. W. H. Weber and J. Lambe, *Appl. Optics.*, 1976, **15**, 2299.
14. R. Reisfeld and S. Neuman, *Nature*, 1978, **274**, 144.
15. R. Reisfeld and Y. Kalisky, *Nature*, 1980, **283**, 281.
16. R. Reisfeld and C. K. Jorgensen, *Struct. Bond.*, 1982, **49**, 1.
17. R. Reisfeld, *Mater. Sci. Eng.*, 1985, **71**, 375.
18. B. C. Rowan, L. R. Wilson and B. S. Richards, *IEEE J. Sel. Top. Quant.*, 2008, **14**, 1312.
19. L. D. Carlos, R. A. S. Ferreira, V. de Zea Bermudez and S. J. L. Ribeiro, *Adv. Mater.*, 2009, **21**, 509.
20. R. Reisfeld, *Opt. Mater.*, 2010, **32**, 850.
21. F. Purcell-Milton and Y. K. Gun'ko, *J. Mater. Chem.*, 2012, **22**, 16687.
22. G. Maggioni, A. Campagnaro, S. Carturan and A. Quaranta, *Sol. Energ. Mat. Sol. C.*, 2013, **108**, 27.
23. L. H. Slooff, E. E. Bende, A. R. Burgers, T. Budel, M. Pravettoni, R. P. Kenny, E. D. Dunlop and A. Büchtemann, *Phys. Status Sol. - R.*, 2008, **2**, 257.
24. A. F. Mansour, H. M. A. Killa, S. Abd El-Wanees and M. Y. El-Sayed, *Polym. Test.*, 2005, **24**, 519.
25. A. F. Mansour, *Polym. Test.*, 1998, **17**, 153.
26. M. G. Debije, P. P. C. Verbunt, B. C. Rowan, B. S. Richards and T. L. Hoeks, *Appl. Optics*, 2008, **47**, 6763.
27. J. C. Goldschmidt, M. Peters, M. Hermle and S. W. Glunz, *J. Appl. Phys.*, 2009, **105**, 114911.
28. K. Bhaumik, J. D. Hurst, P. J. Nadkarni, N. Sankaran and S. Velate, *Luminescent solar collector*, US2010043880, U.S. Patent, 2010.
29. M. Buffa, S. Carturan, M. G. Debije, A. Quaranta and G. Maggioni, *Sol. Energ. Mat. Sol. C.*, 2012, **103**, 114.
30. U. Resch-Genger, M. Grabolle, S. Cavaliere-Jaricot, R. Nitschke and T. Nann, *Nat. Methods*, 2008, **5**, 763.
31. J. A. Levitt and W. H. Weber, *Appl. Optics*, 1977, **16**, 2684.
32. J. S. Batchelder, A. H. Zewail and T. Cole, *Appl. Optics*, 1981, **20**, 3733.
33. A. M. Hermann, *Sol. Energy*, 1982, **29**, 323.
34. M. A. El-Shahawy and A. F. Mansour, *J. Mater. Sci.- Mater. El.*, 1996, **7**, 171.
35. B. A. Swartz, T. Cole and A. H. Zewail, *Opt. Lett.*, 1977, **1**, 73.
36. J. M. Drake, M. L. Lesiecki, J. Sansregret and W. R. L. Thomas, *Appl. Optics*, 1982, **21**, 2945.
37. I. Baumberg, O. Berezin, A. Drabkin, B. Gorelik, L. Kogan, M. Voskobojnik and M. Zaidman, *Polym. Degrad. Stab.*, 2001, **73**, 403.
38. W. G. J. H. M. van Sark, K. W. J. Barnham, L. H. Slooff, A. J. Chatten, A. Büchtemann, A. Meyer, S. J. McCormack, R. Koole, D. J. Farrell, R. Bose, E. E. Bende, A. R. Burgers, T. Budel, J. Quilitz, M. Kennedy, T. Meyer, C. D. M. Donegá, A. Meijerink and D. Vanmaekelbergh, *Opt. Express*, 2008, **16**, 21773.
39. R. Kinderman, L. H. Slooff, A. R. Burgers, N. J. Bakker, A. Buchtemann, R. Danz and J. A. M. van Roosmalen, *J. Sol. Energ.-T. Asme*, 2007, **129**, 277.
40. M. G. Debije, P. P. C. Verbunt, P. J. Nadkarni, S. Velate, K. Bhaumik, S. Nedumbamana, B. C. Rowan, B. S. Richards and T. L. Hoeks, *Appl. Optics*, 2011, **50**, 163.
41. R. Reisfeld, M. Eyal, V. Chernyak and R. Zusman, *Sol. Energ. Mater.*, 1988, **17**, 439.
42. L. R. Wilson and B. S. Richards, *Appl. Optics*, 2009, **48**, 212.
43. G. Seybold and G. Wagenblast, *Dyes Pigments*, 1989, **11**, 303.
44. R. Reisfeld, D. Shamrakov and C. Jorgensen, *Sol. Energ. Mat. Sol. C.*, 1994, **33**, 417.
45. A. F. Mansour, M. G. El-Shaarawy, S. M. El-Bashir, M. K. El-Mansy and M. Hammam, *Polym. Int.*, 2002, **51**, 393.
46. F. Castiglione, G. Lanzani, A. Mele, A. Monguzzi, M. Passarello, A. Ruggirello, F. Scotognella and V. T. Liveri, *J. Mater. Sci.*, 2011, **46**, 6402.

47. D. B. Murphy and M. W. Davidson, *Fundamentals of Light Microscopy and Electronic Imaging*, John Wiley & Sons, Inc., 2013.
48. P. Reiss, M. Protiere and L. Li, *Small*, 2009, **5**, 154.
49. G. V. Shcherbatyuk, R. H. Inman, C. Wang, R. Winston and S. Ghosh, *Appl. Phys. Lett.*, 2010, **96**, 191901.
50. S. J. Gallagher, B. Norton and P. C. Eames, *Sol. Energy*, 2007, **81**, 813.
51. Isnaeni, K. H. Kim, D. L. Nguyen, H. Lim, T. N. Pham and Y. H. Cho, *Appl. Phys. Lett.*, 2011, **98**, 012109.
52. U. Banin, M. Bruchez, A. P. Alivisatos, T. Ha, S. Weiss and D. S. Chemla, *J. Chem. Phys.*, 1999, **110**, 1195.
53. W. G. J. H. M. van Sark, P. L. T. M. Frederix, A. a. Bol, H. C. Gerritsen and A. Meijerink, *ChemPhysChem*, 2002, **3**, 871.
54. M. Nirmal, B. O. Dabbousi, M. G. Bawendi, J. J. Macklin, J. K. Trautman, T. D. Harris and L. E. Brus, *Nature*, 1996, **383**, 802.
55. M. Kuno, D. P. Fromm, H. F. Hamann, A. Gallagher and D. J. Nesbitt, *J. Chem. Phys.*, 2000, **112**, 3117.
56. B. Jezowskatrzebiatowska, E. Lukowiak, W. Strek, A. Buczkowski, S. Patela, J. Radojewski and J. Sarzynski, *Sol. Energ. Mater.*, 1986, **13**, 267.
57. L. M. Shao, J. Q. Zhao, Z. G. Xia and X. P. Jing, *J. Electrochem. Soc.*, 2011, **158**, J300.
58. G. Zucchi, V. Murugesan, D. Tondelier, D. Aldakov, T. Jeon, F. Yang, P. Thuery, M. Ephritikhine and B. Geffroy, *Inorg. Chem.*, 2011, **50**, 4851.
59. O. Moudam, B. C. Rowan, M. Alamiry, P. Richardson, B. S. Richards, A. C. Jones and N. Robertson, *Chem. Commun.*, 2009, 6649.
60. M. M. Nolasco, P. M. Vaz, V. T. Freitas, P. P. Lima, P. S. André, R. A. S. Ferreira, P. D. Vaz, P. Ribeiro-Claro and L. D. Carlos, *J. Mater. Chem. A*, 2013, **1**, 7339.
61. O. L. Malta, H. F. Brito, J. F. S. Menezes, F. R. G. Silva, C. de Mello Donegá and S. Alves Junior, *Chem. Phys. Lett.*, 1998, **282**, 233.
62. P. P. Lima, M. M. Nolasco, F. A. A. Paz, R. A. S. Ferreira, R. L. Longo, O. L. Malta and L. D. Carlos, *Chem. Mater.*, 2013, **25**, 586.
63. D. W. Dong, S. C. Jiang, Y. F. Men, X. L. Ji and B. Z. Jiang, *Adv. Mater.*, 2000, **12**, 646.
64. Y. H. Li, H. J. Zhang, S. B. Wang, Q. G. Meng, H. R. Li and X. H. Chuai, *Thin Solid Films*, 2001, **385**, 205.
65. H. R. Li, L. S. Fu, J. Lin and H. J. Zhang, *Thin Solid Films*, 2002, **416**, 197.
66. P. Lenaerts, A. Storms, J. Mullens, J. D'Haen, C. Gorller-Walrand, K. Binnemans and K. Driesen, *Chem. Mater.*, 2005, **17**, 5194.
67. Y. L. Sui and B. Yan, *J. Photoch. Photobio. A*, 2006, **182**, 1.
68. E. O. Oh, Y. H. Kim and C. M. Whang, *J. Electroceram.*, 2006, **17**, 335.
69. D. Zhao, S. J. Seo and B. S. Bae, *Adv. Mater.*, 2007, **19**, 3473.
70. E. Pecoraro, R. A. Sá Ferreira, C. Molina, S. J. L. Ribeiro, Y. Messsaddeq and L. D. Carlos, *J. Alloy. Compd.*, 2008, **451**.
71. B. Yan, Y. L. Sui and J. L. Liu, *J Alloy Compd*, 2009, **476**, 826.
72. Y. Wang, H. R. Li, Y. Feng, H. J. Zhang, G. Calzaferri and T. Z. Ren, *Angew. Chem., Int. Ed.*, 2010, **49**, 1434.
73. Z. E. Chamas, X. M. Guo, J. L. Canet, A. Gautier, D. Boyer and R. Mahiou, *Dalton Trans.*, 2010, **39**, 7091.
74. H. S. He, M. Dubey, A. G. Sykes and P. S. May, *Dalton Trans.*, 2010, **39**, 6466.
75. L. Armelao, G. Bottaro, S. Quici, C. Scalera, M. Cavazzini, G. Accorsi and M. Bolognesi, *Chemphyschem*, 2010, **11**, 2499.
76. J. Graffion, X. Cattoën, M. Wong Chi Man, V. R. Fernandes, P. S. André, R. A. S. Ferreira and L. D. Carlos, *Chem. Mater.*, 2011, **23**, 4773.
77. J. Graffion, A. M. Cojocariu, X. Cattoën, R. A. S. Ferreira, V. R. Fernandes, P. S. André, L. D. Carlos, M. Wong Chi Man and J. R. Bartlett, *J. Mater. Chem.*, 2012, **22**, 13279.
78. P. P. Lima, R. A. S. Ferreira, R. O. Freire, F. A. A. Paz, L. S. Fu, S. Alves, L. D. Carlos and O. L. Malta, *ChemPhysChem*, 2006, **7**, 735.
79. P. P. Lima, F. A. A. Paz, R. A. S. Ferreira, V. de Zea Bermudez and L. D. Carlos, *Chem. Mater.*, 2009, **21**, 5099.
80. S. Chandra, S. McCormack, J. Doran, M. Kennedy and A. Chatten, *Proceedings of the 25th European Photovoltaic Solar Energy Conference and Exhibition*, Valencia, 2010.
81. S. M. El-Bashir, F. M. Barakat and M. S. AlSalhi, *J. Lumin.*, 2013, **143**, 43.
82. R. Reisfeld, T. Saraidarov, G. Panzer, V. Levchenko and M. Gaft, *Opt. Mater.*, 2011, **34**, 351.
83. M. Fukushima, H. Yanagi, S. Hayashi, N. Suganuma and Y. Taniguchi, *Thin Solid Films*, 2003, **438**, 39.
84. V. Levchenko, M. Grouchko, S. Magdassi, T. Saraidarov and R. Reisfeld, *Opt. Mater.*, 2011, **34**, 360.
85. M. Iosin, P. Baldeck and S. Astilean, *Nucl. Instrum. Meth. B*, 2009, **267**, 403.
86. J. Zhu, K. Zhu and L. Q. Huang, *Phys. Lett. A*, 2008, **372**, 3283.
87. R. Reisfeld, V. Levchenko and T. Saraidarov, *Polym. Advan. Technol.*, 2011, **22**, 60.
88. R. Reisfeld, M. Pietraszkiewicz, T. Saraidarov and V. Levchenko, *J. Rare Earth*, 2009, **27**, 544.
89. R. Reisfeld, T. Saraidarov and V. Levchenko, *J. Sol-Gel Sci. Techn.*, 2009, **50**, 194.
90. T. Saraidarov, V. Levchenko and R. Reisfeld, *Phys. Status Solidi C*, 2010, **7**, 2648.
91. D. Brusilovsky, M. Eyal and R. Reisfeld, *Chem. Phys. Lett.*, 1988, **153**, 203.
92. R. Reisfeld, M. Eyal and D. Brusilovsky, *Chem. Phys. Lett.*, 1988, **153**, 210.

93. J. R. Lakowicz, K. Ray, M. Chowdhury, H. Szmacinski, Y. Fu, J. Zhang and K. Nowaczyk, *Analyst*, 2008, **133**, 1308.
94. J. R. Lakowicz, *Plasmonics*, 2006, **1**, 5.
95. W. G. J. H. M. van Sark, J. de Wild, J. K. Rath, A. Meijerink and R. E. I. Schropp, *Nanoscale Res. Lett.*, 2013, **8**, Art. Number 81.
96. F. Auzel, *Chem. Rev.*, 2004, **104**, 139.
97. F. Wang and X. G. Liu, *Chem. Soc. Rev.*, 2009, **38**, 976.
98. F. Wang, Y. Han, C. S. Lim, Y. H. Lu, J. Wang, J. Xu, H. Y. Chen, C. Zhang, M. H. Hong and X. G. Liu, *Nature*, 2010, **463**, 1061.
99. G. Y. Chen, C. H. Yang and P. N. Prasad, *Accounts Chem Res*, 2013, **46**, 1474.
100. H. Dong, L. D. Sun and C. H. Yan, *Nanoscale*, 2013, **5**, 5703.
101. H. Lian, Z. Hou, M. Shang, D. Geng, Y. Zhang and J. Lin, 2013, **57**.
102. P. Gibart, F. Auzel, J. C. Guillaume and K. Zahraman, *Jpn. J. Appl. Phys.*, 1996, **35**, 4401.
103. B. S. Richards and A. Shalav, *IEEE T. Electron. Dev.*, 2007, **54**, 2679.
104. J. de Wild, J. K. Rath, A. Meijerink, W. G. J. H. M. van Sark and R. E. I. Schropp, *Sol. Energ. Mat. Sol. C.*, 2010, **94**, 2395.
105. M. Liu, Y. Lu, Z. B. Xie and G. M. Chow, *Sol. Energ. Mat. Sol. C.*, 2011, **95**, 800.
106. G. B. Shan and G. P. Demopoulos, *Adv. Mater.*, 2010, **22**, 4373.
107. J. de Wild, A. Meijerink, J. K. Rath, W. G. J. H. M. van Sark and R. E. I. Schropp, *Sol. Energ. Mat. Sol. C*, 2010, **94**, 1919.
108. A. Shalav, B. S. Richards, T. Trupke, K. W. Kra□mer and H. U. Gu□del, *Appl. Phys. Lett.*, 2005, **86**.
109. T. Trupke, A. Shalav, B. S. Richards, P. Wurfel and M. A. Green, *Sol Energ Mat Sol C*, 2006, **90**, 3327.
110. X. D. Zhang, X. Jin, D. F. Wang, S. Z. Xiong, X. H. Geng and Y. Zhao, *Phys. Status Solidi C*, 2010, **7**, 1128.
111. D. F. Wang, X. D. Zhang, Y. J. Liu, C. Y. Wu, C. S. Zhang, C. C. Wei and Y. Zhao, *Chinese Phys. B*, 2013, **22**, 027801.
112. Y. C. Chen and T. M. Chen, *J. Rare Earth*, 2011, **29**, 723.
113. J.-l. Adam, *Chem. Rev.*, 2002, **102**, 2461.
114. C. B. de Araújo, L. S. Menezes, G. S. Maciel, L. H. Acioli, A. S. L. Gomes, Y. Messaddeq, A. Florez and M. A. Aegerter, *Appl. Phys. Lett.*, 1996, **68**, 602.
115. T. Catunda, L. A. O. Nunes, A. Florez, Y. Messaddeq and M. A. Aegerter, *Phys. Rev. B*, 1996, **53**, 6065.
116. G. S. Maciel, C. B. de Araújo, Y. Messaddeq and M. A. Aegerter, *Phys. Rev. B*, 1997, **55**, 6335.
117. L. H. Acioli, J.-T. Guo, C. B. de Araújo, Y. Messaddeq and M. Aegerter, *J. Lumin.*, 1997, **72-74**, 68.
118. C. B. de Araújo, G. S. Maciel, L. S. Menezes, N. Rakov, E. L. Falcão-Filho, V. A. Jerez and Y. Messaddeq, *CR. Chim.*, 2002, **5**, 885.
119. L. de Araújo, A. Gomes, C. de Araújo, Y. Messaddeq, A. Florez and M. Aegerter, *Phys. Rev. B*, 1994, **50**, 16219.
120. I. R. Martín, V. D. Rodríguez, V. Lavín and U. R. Rodríguez-Mendoza, *J. Alloy. Compd.*, 1998, **275-277**, 345.
121. E. Martins, C. B. de Araújo, J. R. Delben, A. S. L. Gomes, B. J. da Costa and Y. Messadeq, *Opt. Commun.*, 1998, **158**, 61.
122. E. Pecoraro, D. F. de Sousa, R. Lebullenger, A. C. Hernandes and L. A. O. Nunes, *J. Appl. Phys.*, 1999, **86**, 3144.
123. W. Lozano, C. B. de Araújo, C. Egalon, A. S. L. Gomes, B. J. Costa and Y. Messadeq, *Opt. Commun.*, 1998, **153**, 271.
124. I. R. Martın, J. Méndez-Ramos, V. D. Rodríguez, J. J. Romero and J. García-Solé, *Opt. Mater.*, 2003, **22**, 327.
125. I. R. Martín, V. D. Rodríguez, V. Lavín and U. R. Rodríguez-Mendoza, *Spectrochim. Acta A*, 1999, **55**, 941.
126. P. Haro-González, I. R. Martín, N. E. Capuj and F. Lahoz, *Opt. Mater.*, 2010, **32**, 1349.
127. H. Q. Wang, M. Batentschuk, A. Osvet, L. Pinna and C. J. Brabec, *Adv. Mater.*, 2011, **23**, 2675.
128. C. Strümpel, M. McCann, G. Beaucarne, V. Arkhipov, A. Slaoui, V. Švrček, C. del Cañizo and I. Tobias, *Sol. Energ. Mat. Sol. C.*, 2007, **91**, 238.
129. J. de Wild, A. Meijerink, J. K. Rath, W. G. J. H. M. van Sark and R. E. I. Schropp, *Energ. Environ. Sci.*, 2011, **4**, 4835.
130. X. C. Ye, J. E. Collins, Y. J. Kang, J. Chen, D. T. N. Chen, A. G. Yodh and C. B. Murray, *Proc. Natl. Acad. Sci. USA*, 2010, **107**, 22430.
131. Y. L. Dai, P. A. Ma, Z. Y. Cheng, X. J. Kang, X. Zhang, Z. Y. Hou, C. X. Li, D. M. Yang, X. F. Zhai and J. Lin, *Acs Nano*, 2012, **6**, 3327.
132. S. Chen, G. H. Zhou, F. F. Su, H. L. Zhang, L. X. Wang, M. J. Wu, M. B. Chen, L. K. Pan and S. W. Wang, *Mater Lett*, 2012, **77**, 17.
133. S. K. W. MacDougall, A. Ivaturi, J. Marques-Hueso, K. W. Krämer and B. S. Richards, *Opt. Express*, 2012, **20**, A879.
134. J. C. Goldschmidt, S. Fischer, P. Löper, K. W. Krämer, D. Biner, M. Hermle and S. W. Glunz, *Sol. Energ. Mat. Sol. C.*, 2011, **95**, 1960.
135. E. Verhagen, L. Kuipers and A. Polman, *Opt. Express*, 2009, **17**, 14586.

136. S. Fischer, F. Hallermann, T. Eichelkraut, G. von Plessen, K. W. Krämer, D. Biner, H. Steinkemper, M. Hermle and J. C. Goldschmidt, *Opt. Express*, 2012, **20**, 271.
137. C. Andriamiadamanana, A. Ferrier, L. Lombez, A. L. Joudrier, N. Naghavi, P. Ghenuche, N. Bardou, J. L. Pelouard, S. Collin, F. Pelle and J. F. Guillemoles, *Proc. SPIE*, 2012, **8256**, Art. number 825608.
138. R. T. Wegh, H. Donker, K. D. Oskam and A. Meijerink, *Science*, 1999, **283**, 663.
139. B. M. van der Ende, L. Aarts and A. Meijerink, *Phys. Chem. Chem. Phys.*, 2009, **11**, 11081.
140. P. Vergeer, T. Vlugt, M. Kox, M. den Hertog, J. van der Eerden and A. Meijerink, *Phys. Rev. B*, 2005, **71**, 014119.
141. L. J. Borrero-Gonzalez, G. Galleani, D. Manzani, L. A. O. Nunes and S. J. L. Ribeiro, *Opt. Mater.*, 2013, **35**, 2085.
142. Y. Xu, X. Zhang, S. Dai, B. Fan, H. Ma, J.-l. Adam, J. Ren and G. Chen, *J. Phys. Chem. C.*, 2011, **115**, 13056.
143. K. Deng, X. Wei, X. Wang, Y. Chen and M. Yin, *Appl. Phys. B-Lasers O.*, 2011, **102**, 555.
144. Q. J. Chen, W. J. Zhang, X. Y. Huang, G. P. Dong, M. Y. Peng and Q. Y. Zhang, *J. Alloy. Compd.*, 2012, **513**, 139.
145. A. Guille, A. Pereira, C. Martinet and B. Moine, *Opt. Lett.*, 2012, **37**, 2280.
146. B. M. van der Ende, L. Aarts and A. Meijerink, *Adv. Mater.*, 2009, **21**, 3073.
147. J. T. van Wijngaarden, S. Scheidelaar, T. J. H. Vlugt, M. F. Reid and A. Meijerink, *Phys. Rev. B*, 2010, **81**, 155112.
148. D. Serrano, A. Braud, J. L. Doualan, P. Camy, A. Benayad, V. Ménard and R. Moncorgé, *Opt. Mater.*, 2011, **33**, 1028.
149. G. Lakshminarayana, H. Yang, S. Ye, Y. Liu and J. Qiu, *J. Phys. D Appl. Phys.*, 2008, **41**, 175111.
150. X. F. Liu, Y. Teng, Y. X. Zhuang, J. H. Xie, Y. B. Qiao, G. P. Dong, D. P. Chen and J. R. Qiu, *Opt. Lett.*, 2009, **34**, 3565.
151. J. J. Eilers, D. Biner, J. T. van Wijngaarden, K. Kra□mer, H. U. Gu□del and A. Meijerink, *Appl. Phys. Lett.*, 2010, **96**, 151106.
152. L. J. Borrero-Gonzalez and L. A. Nunes, *J. Phys. Condens. Mat.*, 2012, **24**, 385501.
153. J. J. Zhou, Y. Teng, S. Ye, G. Lin and J. R. Qiu, *Opt Mater*, 2012, **34**, 901.
154. P. Song and C. Jiang, *AIP Adv.*, 2012, **2**, 042130.
155. P. Escribano, B. Julián-López, J. Planelles-Aragó, E. Cordoncillo, B. Viana and C. Sanchez, *J. Mater. Chem.*, 2008, **18**, 23.
156. K. Binnemans, *Chem. Rev.*, 2009, **109**, 4283.
157. J.-C. G. Bünzli and S. V. Eliseeva, *J. Rare Earth.*, 2010, **28**, 824.
158. S. Sivakumar, P. R. Diamente and F. C. van Veggel, *Chem.- Eur. J.*, 2006, **12**, 5878.
159. S. K. Singh, A. K. Singh and S. B. Rai, *Nanotechnology*, 2011, **22**, 275703.
160. W. Q. Zou, C. Visser, J. A. Maduro, M. S. Pshenichnikov and J. C. Hummelen, *Nat. Photonics*, 2012, **6**, 560.
161. X. J. Xie and X. G. Liu, *Nat. Mater.*, 2012, **11**, 842.
162. M. D. Hughes, C. Maher, D.-A. Borca-Tasciuc, D. Polanco and D. Kaminski, *Renew. Energ.*, 2013, **52**, 266.
163. T. Dienel, C. Bauer, I. Dolamic and D. Bruhwiler, *Sol. Energy*, 2010, **84**, 1366.
164. S. F. H. Correia, P. P. Lima, L. D. Carlos, P. S. André and R. A. S. Ferreira, unpublished work.
165. V. Sholin, J. D. Olson and S. A. Carter, *J. Appl. Phys.*, 2007, **101**, 123114.
166. D. S□ahin, B. Ilan and D. F. Kelley, *J. Appl. Phys.*, 2011, **110**, 033108.
167. K. R. McIntosh, N. Yamada and B. S. Richards, *Appl. Phys. B*, 2007, **88**, 285.
168. R. H. Inman, G. V. Shcherbatyuk, D. Medvedko, A. Gopinathan and S. Ghosh, *Opt. Express*, 2011, **19**, 24308.
169. W. Wu, T. Wang, X. Wang, S. Wu, Y. Luo, X. Tian and Q. Zhang, *Sol. Energy*, 2010, **84**, 2140.
170. O. Y. Edelenbosch, M. Fisher, L. Patrignani, W. G. J. H. M. van Sark and A. J. Chatten, 2013, **21**, A503.
171. J. Bomm, A. Büchtemann, A. J. Chatten, R. Bose, D. J. Farrell, N. L. A. Chan, Y. Xiao, L. H. Slooff, T. Meyer, A. Meyer, W. G. J. H. M. van Sark and R. Koole, *Sol. Energ. Mat. Sol. C.*, 2011, **95**, 2087.
172. V. Misra and H. Mishra, *J. Chem. Phys.*, 2008, **128**, 244701.
173. K. Machida, H. Li, D. Ueda, S. Inoue and G. Adachi, *J. Lumin.*, 2000, **87-9**, 1257.
174. X. Wang, T. Wang, X. Tian, L. Wang, W. Wu, Y. Luo and Q. Zhang, *Sol. Energy*, 2011, **85**, 2179.
175. H. J. Hovel, R. T. Hodgson and J. M. Woodall, *Sol. Energ. Mater.*, 1979, **2**, 19.
176. T. Jin, S. Inoue, K. Machida and G. Adachi, *J. Electrochem. Soc.*, 1997, **144**, 4054.
177. S. M. Geyer, J. M. Scherer, N. Moloto, F. B. Jaworski and M. G. Bawendi, *Acs Nano*, 2011, **5**, 5566.
178. S. D. Hodgson, W. S. M. Brooks, A. J. Clayton, G. Kartopu, V. Barrioz and S. J. C. Irvine, *Nano Energy*, 2013, **2**, 21.
179. T. Fukuda, S. Kato, E. Kin, K. Okaniwa, H. Morikawa, Z. Honda and N. Kamata, *Opt. Mater.*, 2009, **32**, 22.
180. A. C. Pan, C. del Canizo, E. Canovas, N. M. Santos, J. P. Leitão and A. Luque, *Sol. Energ. Mat. Sol. C*, 2010, **94**, 1923.
181. J. Liu, K. Wang, W. Zheng, W. Huang, C. H. Li and X. Z. You, *Prog. Photovoltaics*, 2013, **21**.
182. A. Le Donne, M. Acciarri, D. Narducci, S. Marchionna and S. Binetti, *Prog. Photovoltaics*, 2009, **17**, 519.
183. R. Rothemund, *Sol. Energ. Mat. Sol. C.*, 2014, **120**, 616.

184. P. P. C. Verbunt, A. Kaiser, K. Hermans, C. W. M. Bastiaansen, D. J. Broer and M. G. Debije, *Adv. Funct. Mater.*, 2009, **19**, 2714.
185. C. L. Mulder, P. D. Reusswig, A. M. Velázquez, H. Kim, C. Rotschild and M. A. Baldo, *Opt. Express*, 2010, **18**, A79.
186. C. L. Mulder, P. D. Reusswig, A. P. Beyler, H. Kim, C. Rotschild and M. A. Baldo, *Opt. Express*, 2010, **18**, A91.
187. J. Gjessing, E. S. Marstein and A. Sudbo, *Opt Express*, 2010, **18**, 5481.
188. G. Colantuono, A. Buckley and R. Erdélyi, *J. Lightwave Technol.*, 2013, **31**, 1033.
189. J. Yoon, L. F. Li, A. V. Semichaevsky, J. H. Ryu, H. T. Johnson, R. G. Nuzzo and J. A. Rogers, *Nat. Commun.*, 2011, **2**, Art. number 343.
190. G. Kocher-Oberlehner, M. Bardosova, M. Pemble and B. S. Richards, *Sol. Energ. Mat. Sol. C.*, 2012, **104**, 53.
191. J. W. E. Wiegman and E. van der Kolk, *Sol. Energ. Mat. Sol. C.*, 2012, **103**, 41.
192. B. P. Jelle and C. Breivik, *Energy Procedia*, 2012, **20**, 68.
193. K. Binnemans, P. T. Jones, B. Blanpain, T. Van Gerven, Y. X. Yang, A. Walton and M. Buchert, *J. Clean. Prod.*, 2013, **51**, 1.
194. J. C. G. Bünzli and S. V. Eliseeva, *Chem Sci*, 2013, **4**, 1939.
195. S. V. Eliseeva and J.-C. G. Bünzli, *New J. Chem.*, 2011, **35**, 1165.
196. M. A. de Boer and K. Lammertsma, *ChemSusChem*, 2013, **6**, 2045.

Figure and Table Captions

Fig. 1 Air-Mass 1.5G (AM1.5G) solar irradiance spectrum. The shadowed areas represent the available fraction for DC (26%) and UC (18%) processes for a c-Si wafer. The absorption curves of Si,[197] GaAs[198] and Ge[199] (fraction indicated in parenthesis) are also displayed.

Fig. 2 Schematic representation of the working principle of a LSS and of the main loss mechanisms: 1)Total internal reflection; 2) radiation emitted through the escape cone; 3) re-absorption of the emitted radiation by an optical active centre (solid sphere); 4a) non-absorbed radiation; 4b) non-radiative deactivations; 5a) surface reflection; 5b) self-absorption; 5c) internal waveguide scattering; 5d) surface scattering. Although not represented for simplicity, the photostability of the emitting centres could also be a loss source in LSCs. Photographs of some LSCs under UV irradiation (365 nm) based on (B) a di-ureasil organic-inorganic hybrid doped with $Eu(btfa)_3(MeOH)_2]_2bpta_2$, (btfa=4,4,4-trifluoro-1-phenyl-1,3-butanedione, bpta=trans-1,2-bis(4-pyridil) ethane) and on bipyridine-based bridged silsesquioxanes (C) lacking metal activator centres and doped with (D) Tb^{3+} and (E) Eu^{3+} ions.

Fig. 3 (A) Absorption spectrum of Au-doped PS films and Au/LR305-doped PS waveguides. (B) Emission spectra of Au/LR305(0.001 wt %)-doped samples, excited at 540 nm. The inset shows a photograph of LR305-doped PS-based LSCs. Reproduced from ref.[29] with permission from Elsevier Ltd.

Fig. 4 Excitation (PLE), monitored at (a) 606 nm and (b) 974 nm, and emission (PL),

excited at 482 nm, spectra of Pr^{3+}/Yb^{3+}-doped DC glass layer with different doping concentrations (P0 to P4). Reproduced from ref.[153] with permission from Elsevier Ltd.

Fig. 5 (A) Scheme illustrating IR-806 dye molecules working as antennas for upconverting oleylamine-coated β-$NaYF_4$:Yb,Er NPs. Antenna dyes (green) absorb NIR solar energy (red wavy arrows) and transfer it (brown arrows) to the NPs (in yellow), where UC occurs (the energies of two NIR quanta are summed to emit a quantum of higher energy in the green-yellow region, green-yellow wavy arrow). (B) Emission spectrum of IR-806 in $CHCl_3$ (3.18×10^{-6} M; red line) and absorption spectrum of the oleylamine-coated β-$NaYF_4$:Yb,Er NPs in $CHCl_3$ (green line). OD, optical density. Reproduced from ref.[160] with permission from Nature Publishing.

Fig. 6 Hollow cylinder LSCs of PMMA doped with PbS QDs. Reproduced from ref.[168] with permission from OSA The Optical Society.

Fig. 7 (A) Absorbance and (B) emission spectra of a P(LMA-co-EGDM) plate containing CdSe core/multishell QDs. The inset shows a photograph of the QD-LSC (illuminated by a UV lamp) illustrating the concentrator effect. Reproduced from ref.[171] with permission from Elsevier Ltd.

Fig. 8 Photograph of the LSC attached to a c-Si PV with an emissive organic-inorganic layer of t-U(5000) tri-ureasil doped with $Eu(btfa)_3(MeOH)_2]_2bpta_2$ under (A) room illumination and (B) UV exposure at 365 nm. The scale is 1 cm. (C) Excitation (PLE) and emission (PL) spectra of the hybrid layer.

Fig. 9 (A) Schematic of the DS mechanism in a LDS layer consisting of PbS/CdS core/shell QDs embedded in PMMA and (B) EQE of an InGaAs photodetector covered with the LDS layer. Reproduced from ref. [177] with permission from American Chemical Society.

Fig. 10 Schematic representation of a (A) vertically-aligned LSC[185] and a (B) horizontally-aligned LSC.[186] Reproduced from refs. [185] and [186] with permission from OSA The Optical Society.

Fig. 11 Photograph of the MUSAC museum in Léon, Spain (taken by Olga Cuesta, courtesy of MUSAC, http://www.musac.es/).

Table 1. Optical characteristics of organic-inorganic hybrid materials tested in LSCs.

Table 1

Hybrids	λ_{abs}	λ_p	η_{yield} (%)	η_{Stokes} (%)	η_{opt} (%)	C
Perylimide-GLYMO[44]	420-620	540	98	97	18.8	78
		613	96	94		
Red 305-PS and Red 305/Au NPs-PS[29]	400-580	590	-	95	-	
PbS-PMMA[168]	600-950	750	-	83	6.5	0.271
PbS-toluene- sealed into quartz panels[49]	400-900	870	30	86	1.4	0.154
CdSe/ZnS-toluene- sealed into quartz panels	400-650	625	50	96	0.5	0.06
CdSe/ZnS-toluene- sealed into glass panels[165]	376	623	50	60	0.3	0.05
CdSe-propylene solution	300-650	623	50	60	-	
CdSe/ZnS-polyurethane[50]	560	650	60	86	2.1	0.8
CdSe/CdS/ZnCdS/ZnS/OA-LMA/EGDM[171]	400-650	634	9-45.2	95	15.3	1.91
Tb-PVA/PMMA[172]	280-400	546	40	53	8.8 (290 nm)[a]	1.32
Eu-M6[76]	350	612	34	262	4.3 (350 nm)[a]	0.31
Eu-M4[77]	270	612	8	342	1.2 (290 nm)[a]	0.09
Tb-M4		544	12	274	1.7 (290 nm)[a]	0.13
Eu-tU5[60]	240-450	613	63±6	233	9.0 (360 nm)[a]	0.69
Eu-tU5 [b]	290-380	614	27±3	294	3.2 (360 nm)[a]	0.09
Eu-ormosil[173]	300	610		49	10-15% increase on PV cell efficiency	
AlQ_3/rubrene/DCJTB[9]	450-650	620		87		

GLYMO=3-glycidoxypropyltrimethoxysilane; PMMA=poly(methyl methacrylate); OA=oleic acid; LMA=lauryl methacrylate; EGDM=ethylene glycol dimethacrylate; SA= salicylic acid; PVA=poly(vinylalcohol); M4=bipyridine-based bridged silsesquioxane; tU5= tri-ureasil hybrid matrix; AlQ_3=tris(8-hydroxyquinoline) aluminum; DCJTB=4-(dicyanomethylene)-2-t-butyl-6-(1,1,7,7-tetramethyljulolidyl-9-enyl)-4H-pyran.

[a] η_{opt} calculated by eqn (2).

[b] $Eu(btfa)_3(MeOH)_2]_2bpta_2$.

Figure 1

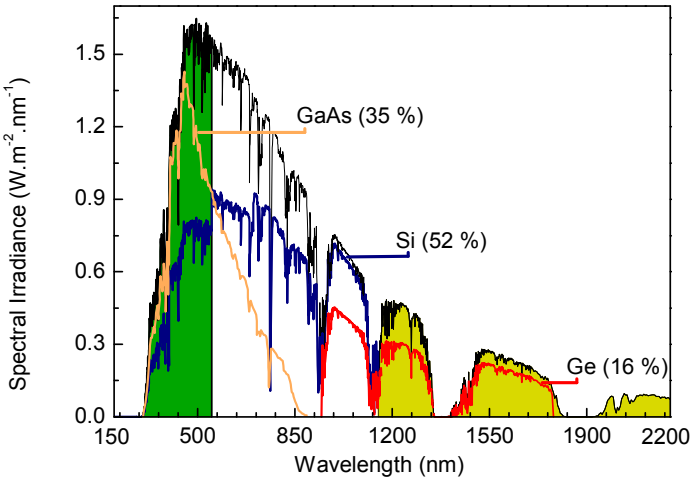

Figure 2

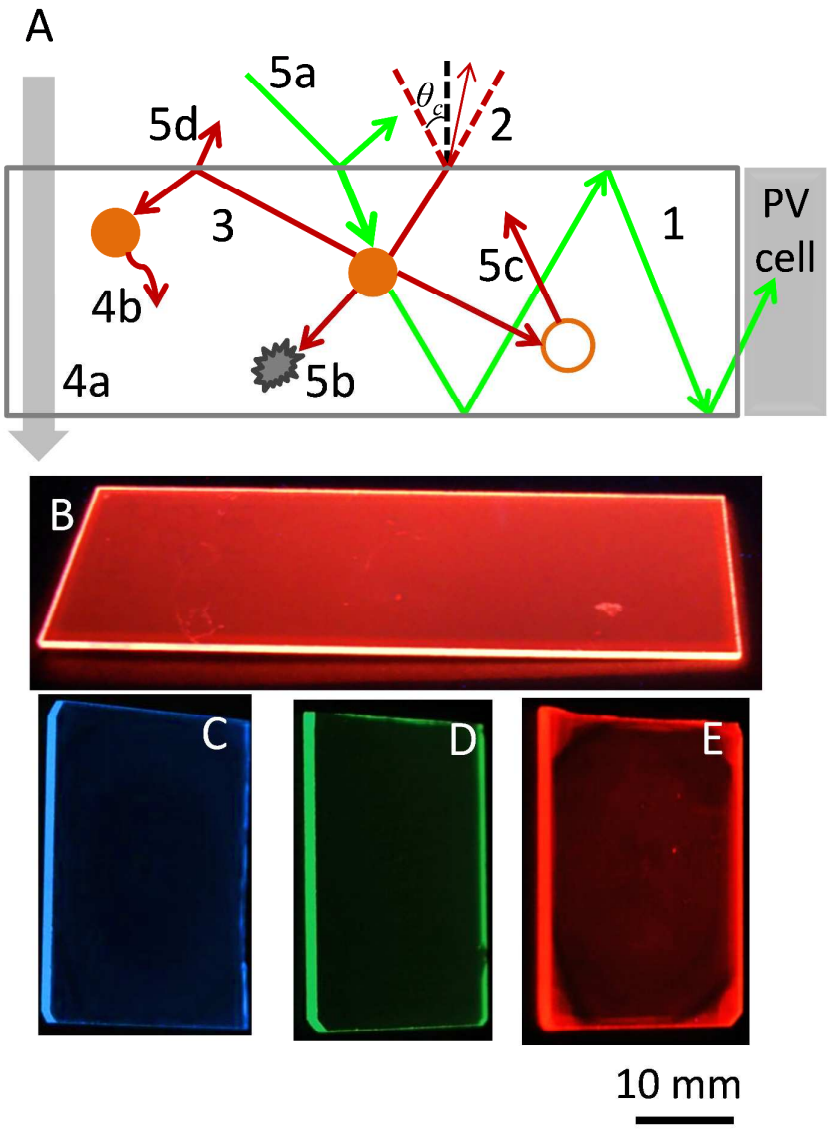

Figure 3

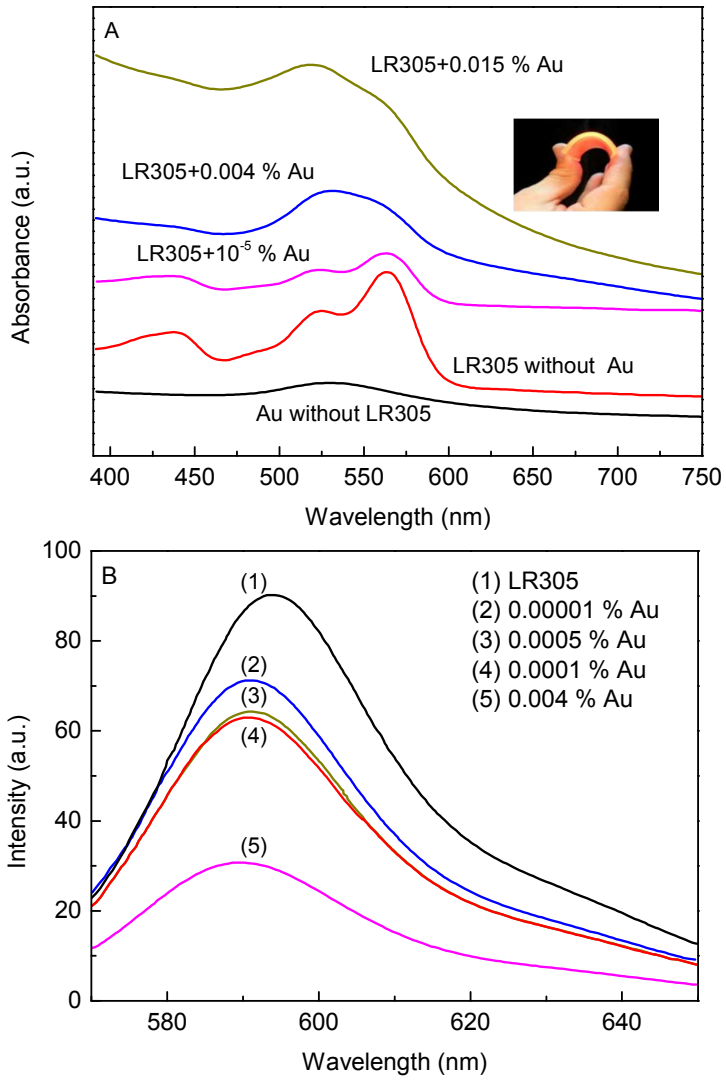

Figure 4

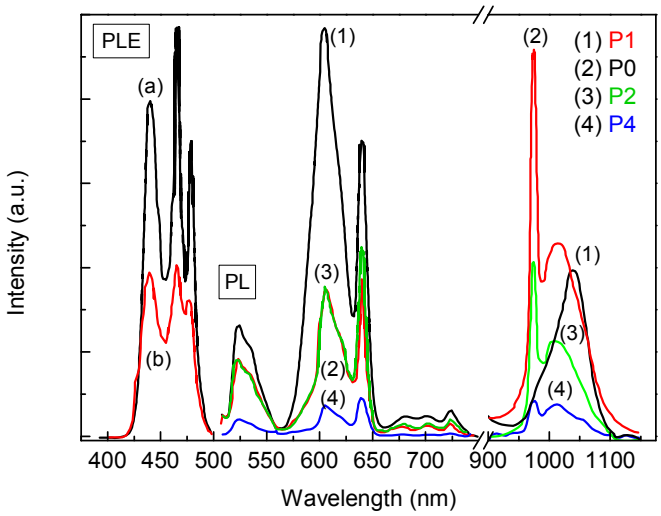

Figure 5

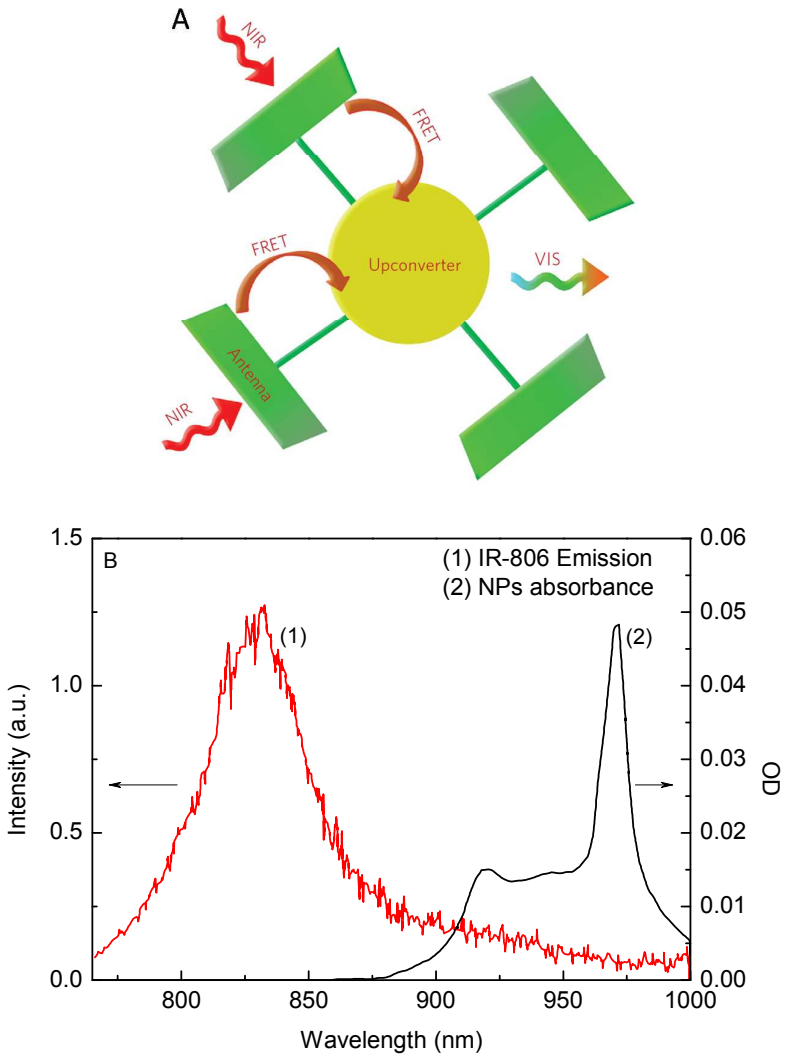

Figure 6

Figure 7

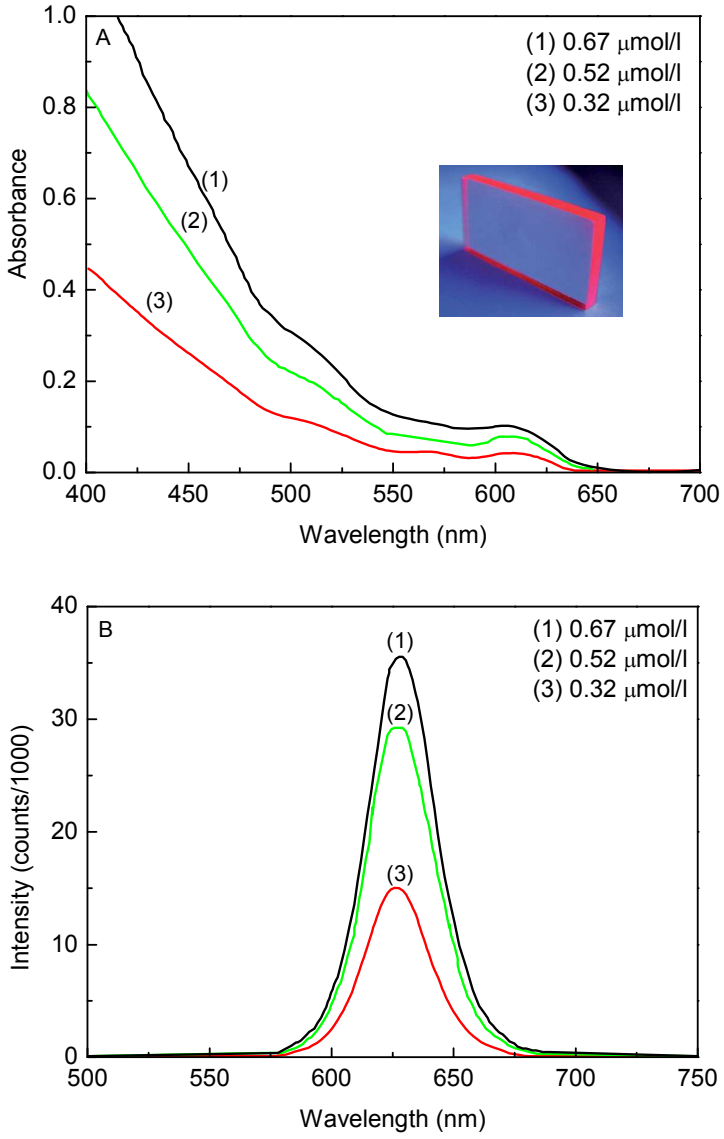

Figure 8

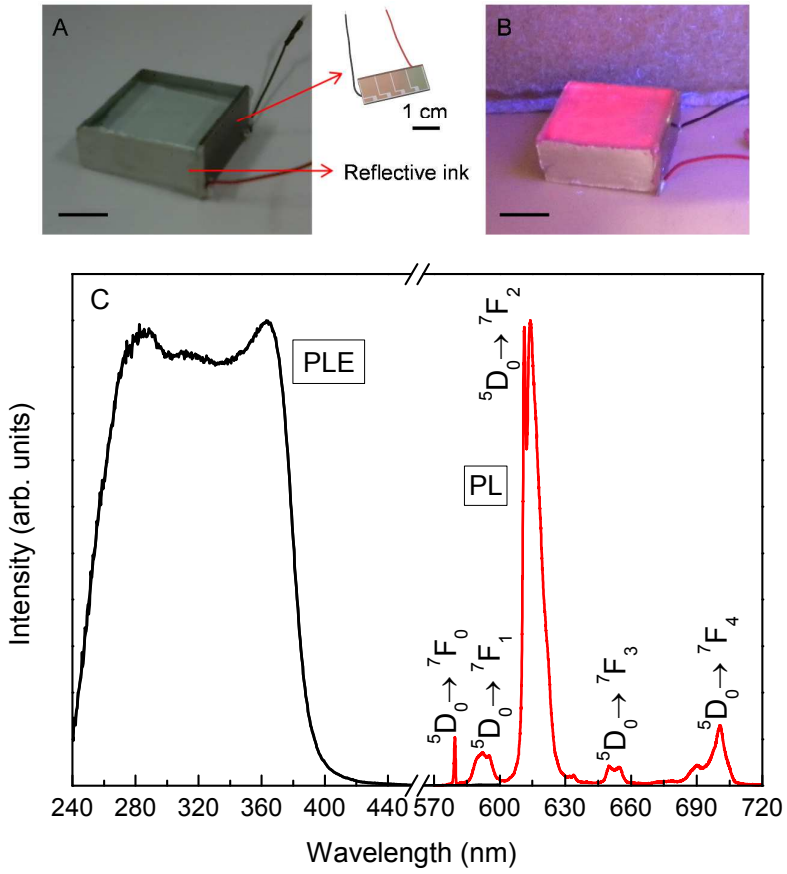

Figure 9

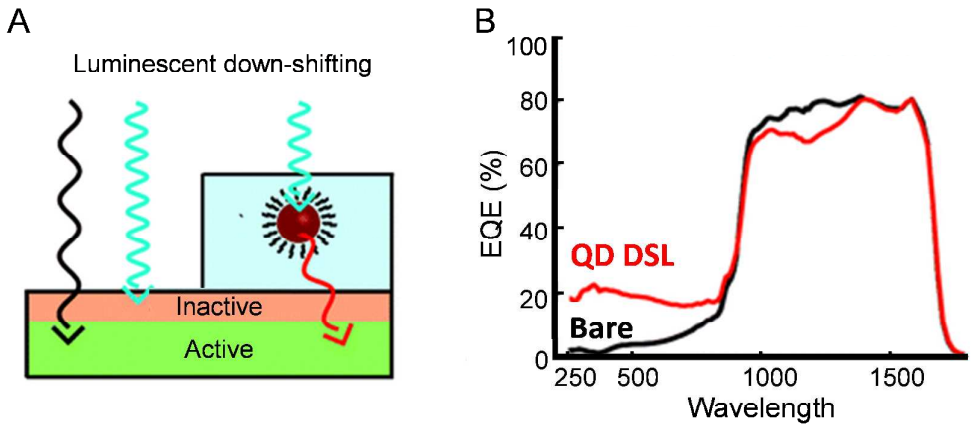

Figure 10

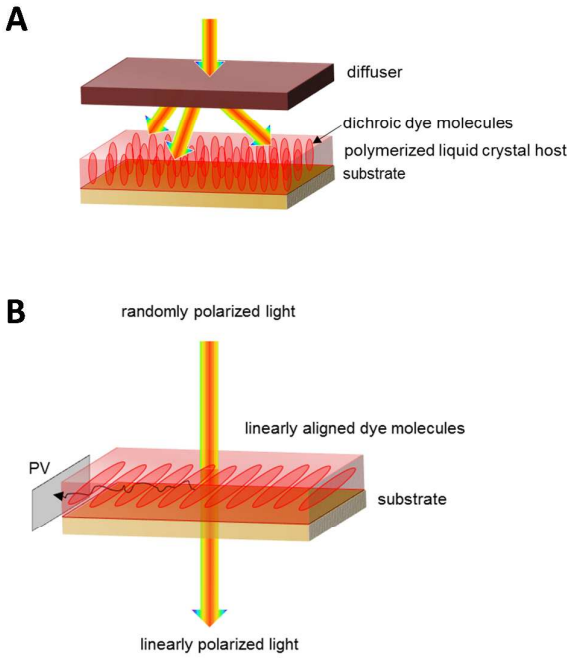

Figure 11